ISTANBUL TECHNICAL UNIVERSITY ★ INSTITUTE OF SCIENCE AND TECHNOLOGY

SOUND PROPAGATION IN TWO-LAYER MEDIA

M.Sc. Thesis by

Sevil Deniz YAKAN, B.Sc.

Department : Ocean Engineering

Programme: Ocean Engineering

JUNE 2007

ISTANBUL TECHNICAL UNIVERSITY ★ INSTITUTE OF SCIENCE AND TECHNOLOGY

SOUND PROPAGATION IN TWO-LAYER MEDIA

M.Sc. Thesis by

Sevil Deniz YAKAN, B.Sc.

508051109

Date of submission : 7 May 2007

Date of defence examination: 11 June 2007

Supervisor (Chairman): Prof. Dr. Serdar BEJİ

Members of the Examining Committee: Prof.Dr. Abdi KÜKNER (İ.T.Ü.)

Prof.Dr. Sedat KAPDAŞLI (İ.T.Ü.)

JUNE 2007

İSTANBUL TEKNİK ÜNİVERSİTESİ ★ FEN BİLİMLERİ ENSTİTÜSÜ

İKİ TABAKALI ORTAMLARDA SESİN YAYILIMI

YÜKSEK LİSANS TEZİ

Müh. Sevil Deniz YAKAN

508051109

Tezin Enstitüye Verildiği Tarih : 7 Mayıs 2007

Tezin Savunulduğu Tarih : 11 Haziran 2007

Tez Danışmanı : Prof.Dr. Serdar BEJİ

Diğer Jüri Üyeleri: Prof.Dr. Abdi KÜKNER (İ.T.Ü.)

Prof.Dr. Sedat KAPDAŞLI (İ.T.Ü.)

HAZİRAN 2007

FOREWORD

First, I want to thank to my thesis advisor Prof. Dr. Serdar Beji for his suggestions about the thesis subject. His guidance helped me to complete this study.

I also thank to Captain Şeyhmus Direk for providing me the oceanographic data used in the codes.

Next thanks go to my friends Çiğdem Akan, Deniz Bayraktar, Emre Peşman and Burak Karacık for their support and cheering me up.

A special thanks goes to Serdar Aytekin Köroğlu for his warnings and help in the correction of the format mistakes.

Another special thanks goes to Doruk Dündar for his understanding, listening my problems and trying to cheer me up always.

And I want to thank my family, my sister Seçil Öznur and my parents Pembegül and Ahmet very much indeed. They never quit supporting me whatever I do and try to do their best. I know that it is my fortunate to have a family like them.

May 2007 Sevil Deniz Yakan

CONTENTS

FIGURE LIST

SYMBOL LIST

$\mathbf{c}$	: Speed of sound
$\boldsymbol{\theta}$	: Grazing / azimuthal angle
$\boldsymbol{\alpha}$	: Vertical angle
$\mathbf{R}$	: Reflection coefficient
$\mathbf{z}$	: Acoustic impedance
$\mathbf{T}$	: Transmission coefficient
$\mathbf{p_i}$	: Incident acoustic pressure
$\mathbf{p_r}$	: Reflected acoustic pressure
$\mathbf{p_t}$	: Transmitted acoustic pressure
$\mathbf{T}$	: Temperature
$\mathbf{p}$	: Pressure
$\mathbf{S}$	: Salinity
$\mathbf{z}$	: Depth
$\boldsymbol{\Phi}$	: Potential function
$\mathbf{t}$	: Time
$\boldsymbol{\phi}$	: Time-independent potential function
$\boldsymbol{\omega}$	: Angular frequency of the source
$\mathbf{k}$	: Wave number
$\boldsymbol{\lambda}$	: Wave length
$\mathbf{r}$	: Radial distance from the source
$\boldsymbol{\tau}$	: Wave front

İKİ TABAKALI ORTAMLARDA SESİN YAYILIMI

ÖZET

Bu çalışmada, iki tabakalı sualtı ortamlarında ses dalgalarının yayılımı incelenmektedir. Burada iki tabaka ifadesi ortamın iki farklı yoğunluğunu belirtmektedir. Sualtı ortamında sesin yayılımını açıklamak amacıyla öncelikle ses kırılması ve ses yansıması gibi temel kavramlar açıklanmaktadır. Ses yayılım yollarının iki temel parametresi olan ses hızı ve sualtı akustik çevresi belirtilmekte ve ses hızı ile oşinografi parametreleri olan T, sıcaklık, S, tuzluluk, p, basınç arasındaki ilişki vurgulanmaktadır. Yedi farklı ampirik formül kullanılarak ses hızı hesaplamaları gerçekleştirilmekte, birbirleriyle karşılaştırılarak sonuçların yakın olduğu gözlenmektedir. 4. Bölümde ses yayılım modelleri ve akustik yayılım modelleri formüllerinin başlangıç noktası olan dalga denklemi hakkında genel bilgi verilmektedir. Son bölümde, bu yayılım modellerinden biri olan ışın teorisi tanımlanmaktadır. Işın teorisi modellerinin temeli olan ışın izleme metodu ve hesaplamaları açıklanarak İstanbul Boğazı için oniki aylık bir döneme karşı gelen ses hızı profilleri kullanılarak sayısal uygulamalar yapılmaktadır. Işın izleme metodunun sayısal uygulamasında 2005 ve 2006 yıllarına ait ses hız profili verileri kullanılmıştır. Veriler, Seyir Hidrografi ve Oşinografi Dairesi Başkanlığı'ndan alınmıştır ve oradan ölçümler İstanbul Boğazı'nda Beykoz ve Çubuklu mevkileri arasından elde edilmiştir. Işın izleme bilgisayar kodunda rastgele derinliklere birer kaynak ve alıcı yerleştirilmiş ve belirtilen alıcı menzilinde birbirleri arasındaki yayılım yolları elde edilmiştir.

SOUND PROPAGATION IN TWO-LAYER MEDIA

SUMMARY

In this study, the propagation of sound waves in two-layer underwater media is examined. Here, two-layer term signifies the two different densities of the medium. In order to explain sound propagation in underwater medium, firstly basic concepts such as sound refraction and sound reflection are explained. Two main parameters of sound propagation paths which are the speed of sound and the underwater acoustic environment are examined and the relationship between the speed of sound and the oceanographic parameters, T, temperature, S, salinity and p, pressure, are emphasized. Using seven different emprical formulas, sound speed calculations are performed and compared with each other. The results are observed to be quite close. General information about sound propagation models and the wave equation, which is the starting point of the formulations of the acoustic propagation models, is given in section 4. In the last section, one of these propagation models, ray theory is described. Ray tracing method, which is the basis of theoretical ray models, and its computational procedure is explained and numerical applications are done by using various sound speed profiles for the Bosphorus Strait for a period of twelve months. In the numerical applications of ray tracing method, sound speed profile data for the years of 2005 and 2006 are used. The data is taken from the Turkish Navy Office of Navigation, Hydrography and Oceanography. The measurements used for the calculations were taken within the area of Beykoz and Çubuklu in the Istanbul Strait. In the computer code of ray tracing, both a source and a receiver are placed at arbitrary depths, and the propagation paths between these are obtained within a specified range to the receiver.

1. INTRODUCTION

Studies relevant to the propagation of acoustic waves in water are categorized as underwater acoustics. Since it is a broad subject, different science branches are closely related in underwater acoustics. In this study we approach the subject from the physical oceanographic point of view and consider the sound propagation in two-layered media.

The principal aim of this study is to examine underwater sound propagation in a medium of changing sound speed using the method of ray tracing numerically. In section 2, the necessity of using sound waves in water is emphasized and the refraction, reflection, and transmission properties of sound waves are described. In section 3, the variation of the speed of sound due to the principal oceanographic parameters is explained and the basic sound propagation paths are given. The calculation of the speed of sound by using different emprical formulas due to Medwin (1975), Mackenzie (1981), Coppens (1981), Chen-Millero (1977), Leroy (1969), Wilson (1960) and Del Grosso (1974) are compared with each other. In section 4, different sound propagation modeling approaches are mentioned and classified as ray theory, normal mode approach, multipath expansion, fast field approach and parabolic equation techniques. Within these, ray theory and the parabolic equation technique are the range dependent models, and the rest are range independent models, which indicate that the properties change only with depth. In section 5, one of the sound propagation models mentioned in section 4 is re-considered as the basis of this work; namely, the ray tracing. Ray tracing is a mathematical method of following the paths of sound waves. Ray tracing equations are derived from the Helmholtz equation as a second-order differential equation for use in ray tracing computer code. By using this computer code, sound propagation paths are obtained for various sound speed profiles for the Bosphorus Strait for a period of twelve months.

Understanding the propagation of sound is essentially to understand the propagation paths. In order to obtain sound propagation paths ray tracing may be used conveniently in many circumstances. Ray tracing is an essential tool which basically follows the motion of sound as segmented beams. With ray tracing, sound shadows (inaccessible fields of sound waves) and refraction can be observed easily. But, it is an essential point that ray theory is used only if the diffraction is ignored and diffraction can be ignored only if the obstacles encountered are small compared to the wavelength of the sound.

2. UNDERWATER ACOUSTICS

In underwater acoustics, the water is used as the propagation medium, and the basic medium quantities are the speed of sound and the density [1]. Sound is propagated as a longitudinal wave which means that the motion of particles conveying the wave is parallel to the direction of propagation [2]. In the sea it is essential to use sound waves because of their long-distance propagation ability. No other means of transmission – such as light or other kind of electromagnetic waves – can propagate much in the water.

The sea is not perfectly homogeneous and is bounded above and below by some sort of interfaces, so at first, refraction, reflection and transmission properties of sound waves are examined. We begin with the phenomenon of refraction; namely, deflection of a sound beam due to change in the speed of sound.

2.1 Sound Refraction

Refraction is the term used to express the bending of wave rays due to the changing speed of propagating sound wave. Since the speed of sound depends on the temperature T, pressure p and salinity S, change in these parameters causes a change in the speed of propagation of sound, hence refraction. Wave refraction is expressed by Snell's Law.

$$\frac{c_1}{\cos\theta_1} = \frac{c_2}{\cos\theta_2} = \text{constant} \qquad \textbf{(2.1a)}$$

$$\frac{c_1}{\sin\alpha_1} = \frac{c_2}{\sin\alpha_2} = \text{constant} \qquad \textbf{(2.1b)}$$

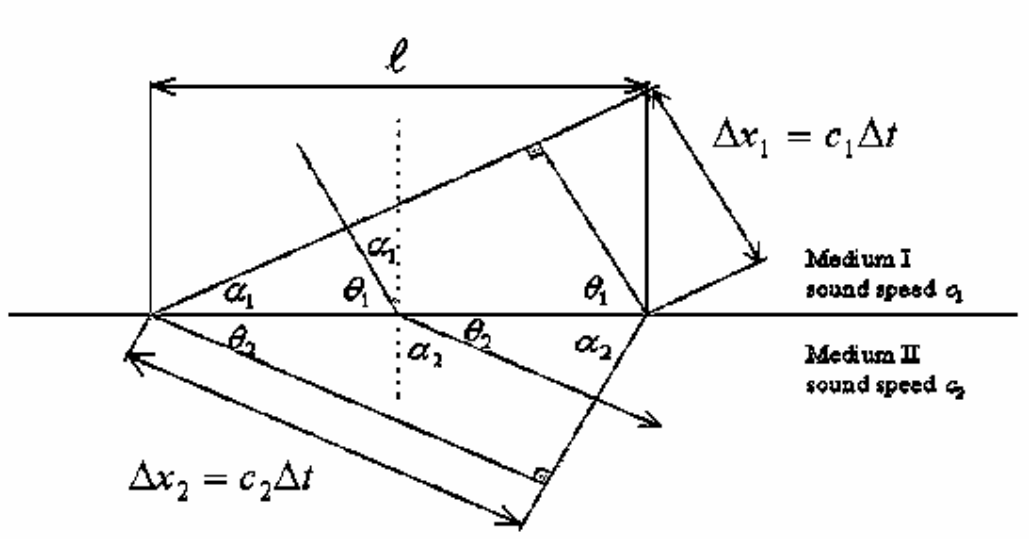

Figure 2.1: Angles and velocities in two-layered media.

From Figure 2.1, using the trigonometric identities, one obtains

$$\left.\begin{aligned} \sin\alpha_1 &= \frac{\Delta x_1}{\ell} = \frac{c_1 \Delta t}{\ell} \\ \sin\alpha_2 &= \frac{\Delta x_2}{\ell} = \frac{c_2 \Delta t}{\ell} \end{aligned}\right\} \qquad \frac{\sin\alpha_1}{c_1} = \frac{\sin\alpha_2}{c_2} = \frac{\Delta t}{\ell} \;\Rightarrow\; \frac{c_1}{\sin\alpha_1} = \frac{c_2}{\sin\alpha_2},$$

which is Snell's law.

The diagram shows two different layers in which the sound velocities are c_1 and c_2, respectively where $c_1 < c_2$ and $\Delta x_1 < \Delta x_2$. The symbol θ refers to the grazing angle and α represents the vertical angle.

An important rule is the tendency of a wave ray to turn towards the velocity minimum. This is clearly seen in the wave refraction diagram where c_1 is smaller than c_2.

By using Snell's Law, the quantity of refraction of a wave ray can be calculated in a medium with velocity change. This is done by rearranging Snell's Law in terms of grazing angle θ.

$$\theta_2 = \cos^{-1}\left[\frac{c_2 \cos\theta_1}{c_1}\right] \qquad \textbf{(2.2)}$$

Basically, sound can be thought as a straight-line ray which bounces up and down between the sea surface and the bottom, while moving away from the source. As seen from the Snell's Law, sound rays have a tendency to bend away from warm waters which have a higher c velocity value, and this causes complex sound propagation patterns.

2.2 Sound Reflection

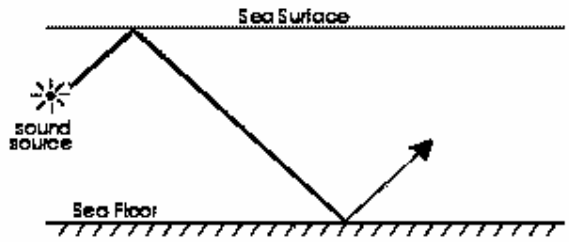

Figure 2.2: Simple reflection ray diagram.

Reflection is the term used to define the process of return of all or a part of a sound beam in the case of encountering a boundary between two media. In the reflection process, the angle of incidence and the angle of reflection are equal to each other. A simple reflection ray diagram is seen in Figure 2.2 [3]. The symbol R is used to express the reflection coefficient. Another important term is the acoustic impedance z and defined as the product of the density and the sound speed of the medium, $z = \rho c$.

An expression for reflection coefficient including acoustic impedance can be written as:

$$R = \frac{(z_2 / z_1) - \sqrt{1 - [n-1]\tan^2 \alpha_i}}{(z_2 / z_1) + \sqrt{1 - [n-1]\tan^2 \alpha_i}} \qquad \textbf{(2.3)}$$

In the expression, $n = (c_2 / c_1)^2$ and α_i is the angle of incidence of the wave ray. An explanatory diagram for both reflected and refracted rays is seen below:

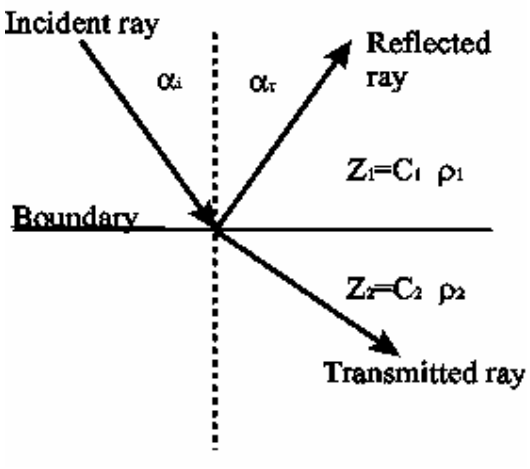

Figure 2.3: Incident reflected and transmitted ray diagram in two-layered media.

The value of reflection coefficient varies between -1 and +1 according to the acoustic impedance values of the mediums.

If $z_2 >> z_1$, $R \Rightarrow 1$. In this case, the boundary is considered as a rigid boundary and most of the acoustic energy will be reflected without a change in phase.

If $z_2 << z_1$, $R \Rightarrow -1$. In this case, the boundary is considered as a soft or pressure release boundary and most of the acoustic energy is reflected with a 180 degree phase change.

If $z_1 = z_2$, $R = 0$. In this case there is no reflection [4].

Examples to the above situations can be given as solid bottom, sea surface, and transmission in unchanging acoustic impedance z, respectively.

Considering the diagram above, reflection and transmission coefficients can also be written via acoustic pressures as

$$p_i = e^{ik_1(x\cos\theta_1 + z\sin\theta_1)} \quad \text{where} \quad k_1 = \frac{\omega}{c_1} \tag{2.4}$$

$$p_r = \mathrm{Re}^{ik_1(x\cos\theta_1 - z\sin\theta_1)} \tag{2.5}$$

$$p_t = Te^{ik_2(x\cos\theta_2 + z\sin\theta_2)} \quad \text{where} \quad k_2 = \frac{\omega}{c_2} \tag{2.6}$$

where p_i is the incident, p_r is the reflected, and p_t is the transmitted acoustic pressure. The common multiplier $e^{i\omega t}$ has been omitted.

In the equations above, it is assumed that incident plane wave has unit amplitude and the amplitudes of reflected and transmitted waves are expressed by *R* and *T* symbols, respectively.

Besides Snell's law, continuity of pressure and vertical particle velocity across the interface at z=0 are the boundary conditions which are used to obtain *R*, *T*, θ_2 quantities.

In medium 1, $p_1 = p_i + p_r$; and in medium 2, $p_2 = p_t$. These are the expressions of total pressure in the mediums. By using these total acoustic pressure expressions, the boundary conditions can be stated as

$$p_1 = p_2 \qquad \textbf{(2.7a)}$$

$$\frac{1}{i\omega\rho_1}\frac{\partial p_1}{\partial z} = \frac{1}{i\omega\rho_2}\frac{\partial p_2}{\partial z} \qquad \textbf{(2.7b)}$$

From the continuity of pressure between two different mediums $p_1 = p_2$ at z=0, we obtain

$$1 + R = Te^{[i(k_2\cos\theta_2 - k_1\cos\theta_1)x]} \qquad \textbf{(2.8)}$$

In the above equation, Snell's law of refraction ($k_2\cos\theta_2 = k_1\cos\theta_1$) which states the invariability of the horizontal component of the wave vector across the interface, is also seen. Because the left side of the equation (2.8) is independent of *x*, the right side of the same equation must also be independent of *x*, and the equation (2.8) is written as

$$1 + R = T \qquad \textbf{(2.9)}$$

3. UNDERWATER SOUND PROPAGATION IN A MEDIUM OF CHANGING SOUND SPEED

Sound propagation in underwater is closely related to sound speed whose parameters are temperature, pressure, and salinity. Hence, variations in these parameters cause variations in sound speed both spatially (with depth / geographically) and temporally (daily / seasonally). Because the gradients in T, p, and S are much more smaller in horizontal direction, the variation in sound speed in the horizontal direction is ignored.

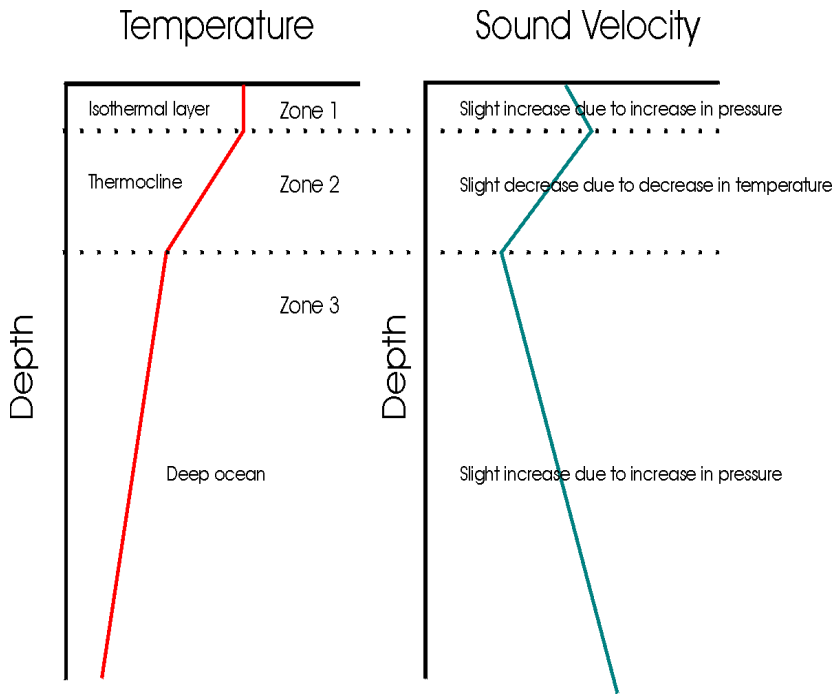

Figure 3.1: Temperature-depth and sound speed-depth profiles.

As an example, temperature-depth and sound speed-depth profiles which are divided into three distinct zones are shown above. In zone 1, which is the closest to the surface, there is an isothermal layer. Mixing of wind and waves forms this isothermal layer and in this layer, sound speed increases because of the increasing pressure. In zone 2, which is thermocline, sound speed decreases because of the decreasing

temperature. In zone 3, which is the deepest region, sound speed increases because of the increasing pressure although temperature is decreasing [5].

3.1 Ocean Acoustic Environment

The properties of the oceanographic environment are the main factors determining the sound speed structure and the acoustic properties of the ocean such as the propagation paths [1].

These propagation paths are mainly classified as (A) direct path, (B) surface duct, (C) bottom bounce, (D) convergence zone, (E) deep sound channel, and (F) reliable acoustic path. These variations occur due to the sound speed structure in the water column and the source-receiver geometry. They are shown in the figures below with the letters A-F, respectively. Combinations of these basic paths can also be obtained [6].

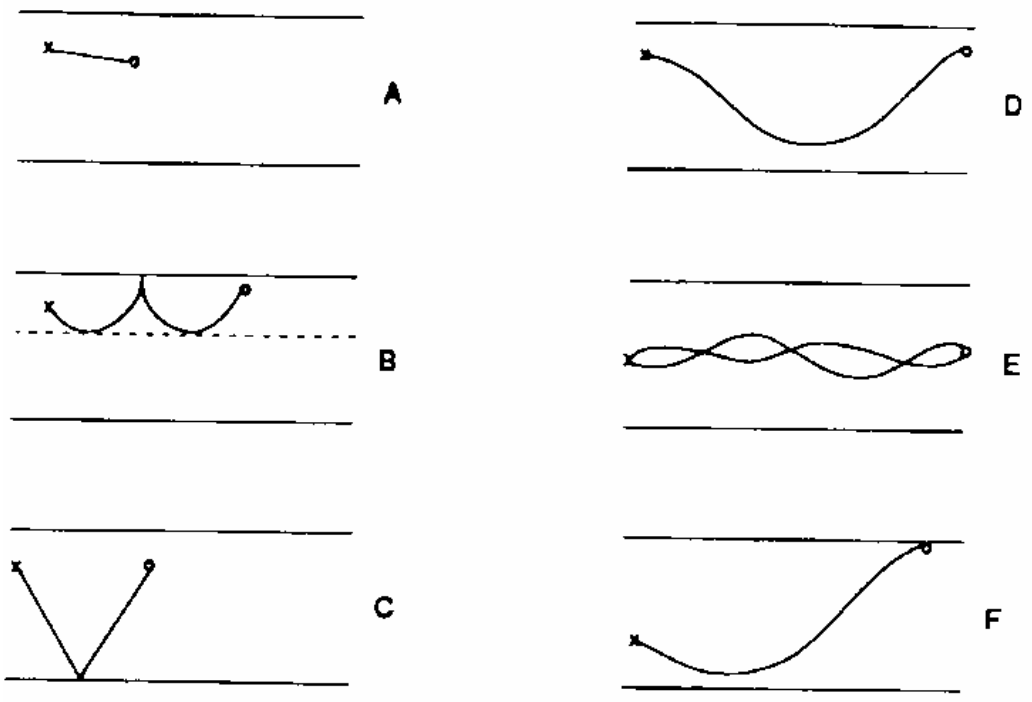

Figure 3.2: Basic propagation paths in the sea.

3.2 Sound Speed in the Sea

Temperature (T), pressure (p) and salinity(S) are the parameters, which cause variations in the sound speed in water [7]. Pressure p is a function of depth z, an

empirical formula containing temperature, salinity and depth for the speed of sound is given by:

$$c = 1449.2 + 4.6T - 0.055T^2 + 0.00029T^3 + (1.34 - 0.01T)(S - 35) + 0.016z \qquad \textbf{(3.1)}$$

This formula is used within the range 0 to 35°C, 0 to 45ppt, and 0 to 1000m, according to Medwin [8].

Besides above empirical formula, many other empirical formulas have been developed for the calculation of sound speed. For instance, a formula given by Mackenzie is:

$$\begin{aligned} c = {} & 1448.96 + 4.591T - 5.304*10^{-2}T^2 + 2.374*10^{-4}T^3 + 1.340(S-35) \\ & + 1.630*10^{-2}z + 1.675*10^{-7}z^2 - 1.025*10^{-2}T(S-35) - 7.139*10^{-13}Tz^3 \end{aligned} \qquad \textbf{(3.2)}$$

This formula is used within the range -2 to 30°C, 25 to 40ppt, and 0 to 8000m [9].

Formula given by Coppens within the range 0 to 30°C, 0 to 40ppt, and 0 to 4000m is:

$$c(0,S,t) = 1449.05 + 45.7t - 5.2t^2 + 0.23t^3 + \left(1.333 - 0.126t + 0.009t^2\right)(S-35)$$

$$\begin{aligned} c(D,S,t) = {} & c(0,S,t) + (16.23 + 0.253t)D + (0.213 - 0.1t)D^2 + \\ & [0.016 + 0.0002(S-35)](S-35)tD \end{aligned} \qquad \textbf{(3.3)}$$

where $t = T/10$ and $D = z/1000$ [10].

Formula given by Chen and Millero within the range 0 to 40°C, 0 to 40ppt, and 0 to 1000bar is [11, 12]:

$$c(S,T,P) = Cw(T,P) + A(T,P)S + B(T,P)S^{3/2} + D(T,P)S^2 \qquad \textbf{(3.4)}$$

where

$$Cw(T,P)=\begin{pmatrix}1402.388+5.0383T-5.8109*10^{-2}T^2+3.3432*10^{-4}T^3\\-1.47797*10^{-6}T^4+3.1419*10^{-9}T^5\end{pmatrix}+$$
$$\begin{pmatrix}0.153563+6.8999*10^{-4}T-8.1829*10^{-6}T^2\\+1.3632*10^{-7}T^3-6.126*10^{-10}T^4\end{pmatrix}P+$$
$$\begin{pmatrix}3.126*10^{-5}-1.7111*10^{-6}T+2.5986*10^{-8}T^2\\-2.5353*10^{-10}T^3+1.0415*10^{-12}T^4\end{pmatrix}P^2+$$
$$\left(-9.7729*10^{-9}+3.8513*10^{-10}T-2.3654*10^{-12}T^2\right)P^3$$

$$A(T,P)=\begin{pmatrix}1.389-1.262*10^{-2}T+7.166*10^{-5}T^2\\+2.008*10^{-6}T^3-3.21*10^{-8}T^4\end{pmatrix}+$$
$$\begin{pmatrix}9.4742*10^{-5}-1.2583*10^{-5}T-6.4928*10^{-8}T^2\\+1.0515*10^{-8}T^3-2.0142*10^{-10}T^4\end{pmatrix}P+$$
$$\begin{pmatrix}-3.9064*10^{-7}+9.1061*10^{-9}T\\-1.6009*10^{-10}T^2+7.994*10^{-12}T^3\end{pmatrix}P^2+$$
$$\left(1.1*10^{-10}+6.651*10^{-12}T-3.391*10^{-13}T^2\right)P^3$$

$$B(T,P)=-1.922*10^{-2}-4.42*10^{-5}T+\left(7.3637*10^{-5}+1.795*10^{-7}T\right)P$$

$$D(T,P)=1.727*10^{-3}-7.9836*10^{-6}P$$

Formula given by Leroy within the range -2 to 34°C, approximately 20 to 42ppt, and all depth in meters is:

$$c=c_0+c_a+c_b+c_c+c_d \qquad \textbf{(3.5)}$$

where

$$c_a=10^{-1}\zeta^2+2*10^{-4}\zeta^2(T-18)^2+10^{-1}\zeta(\phi/90)$$

$$c_b=2*10^{-7}T(T-10)^4$$

$$c_c=5*10^{-4}\zeta^2(\zeta-6)^2$$

$$c_d=1.5*10^{-3}(S-35)^2(1-\zeta)$$

$$c_0 = 1492.9 + 3(T-10) - 6*10^{-3}(T-10)^2 - 4*10^{-2}(T-18)^2 + 1.2(S-35) - 10^{-2}(T-18)(S-35) + z/61$$

and $\zeta = z/1000$. In the above equations, c_0 can be seen as a simplified formula, $c_0 + c_a + c_b$ as a basic formula, and finally c_c and c_d are the corrections for the depths greater than 7000m and salinity lower than 30ppt. Additionally, the depth dependence in c_d is to fit Black Sea conditions [13].

Formula given by Wilson within the range -4 to 30°C, 0 to 37ppt, and 1 to 1000kg/cm^2 is [14]:

$$c = 1449.14 + V_t + V_p + V_s + V_{stp} \quad \textbf{(3.6)}$$

where

$$V_t = 4.5721T - 4.4532*10^{-2}(T^2) - 2.6045*10^{-4}(T^3) + 7.9851*10^{-6}(T^4)$$

$$V_p = 1.60272*10^{-1}P + 1.0268*10^{-5}P^2 + 3.5216*10^{-9}(P^3) + 3.3603*10^{-12}(P^4)$$

$$V_s = 1.39799(S-35) + 1.69202*10^{-3}(S-35)^2$$

$$V_{stp} = (S-35)\begin{pmatrix} -1.1244*10^{-2}T + 7.7711*10^{-7}T^2 + 7.7016*10^{-5}P \\ -1.2943*10^{-7}P^2 + 3.158*10^{-8}PT + 1.579*10^{-9}PT^2 \end{pmatrix} + P(-1.8607*10^{-4}T + 7.4812*10^{-6}T^2 + 4.5283*10^{-8}T^3) + P^2(-2.5294*10^{-7}T + 1.8563*10^{-9}T^2) + P^3(-1.9646*10^{-10}T)$$

Formula given by Del Grosso within the range 0 to 30°C, 30 to 40ppt, and 0 to 1000kg/cm^2 is [15, 16]:

$$c = c_{000} + \Delta c_t + \Delta c_s + \Delta c_p + \Delta c_{stp} \quad \textbf{(3.7)}$$

where

$$c_{000} = 1402.392$$

$$\Delta c_t = 0.501109398873 * 10^{1} T - 0.55094684317 * 10^{-1} \left(T^2\right) + 0.22153596924 * 10^{-3} \left(T^3\right)$$

$$\Delta c_s = 0.132952290781 * 10^{1} S + 0.128955756844 * 10^{-3} S^2$$

$$\Delta c_p = 0.156059257041 P + 0.244998688441 * 10^{-4} P^2 - 0.883392332513 * 10^{-8} P^3$$

$$\begin{aligned}\Delta c_{stp} = & -0.127562783426 * 10^{-1} TS + 0.635191613389 * 10^{-2} TP + \\ & 0.265484716608 * 10^{-7} T^2 P^2 - 0.159349479045 * 10^{-5} TP^2 + \\ & 0.522116437235 * 10^{-9} TP^3 - 0.438031096213 * 10^{-6} PT^3 - \\ & 0.161674495909 * 10^{-8} S^2 P^2 + 0.96840315641 * 10^{-4} ST^2 + \\ & 0.485639620015 * 10^{-5} TPS^2 - 0.340597039004 * 10^{-3} TSP\end{aligned}$$

When using these formulas, their validity range regarding the temperature, salinity, and pressure (depth) should be observed.

Below, an example for the sound speed profile calculated with the formulas given above is shown. The other figures are given in the appendix A section. Calculations are done by taking the statistical mean of the temperature, salinity and depth data between 2005 and 2006 years, and the data are for the stations between the Beykoz and Çubuklu zone in the Istanbul Strait. The measurements were not taken at the same point, and this causes depth differences between 50m to 67m for different months.

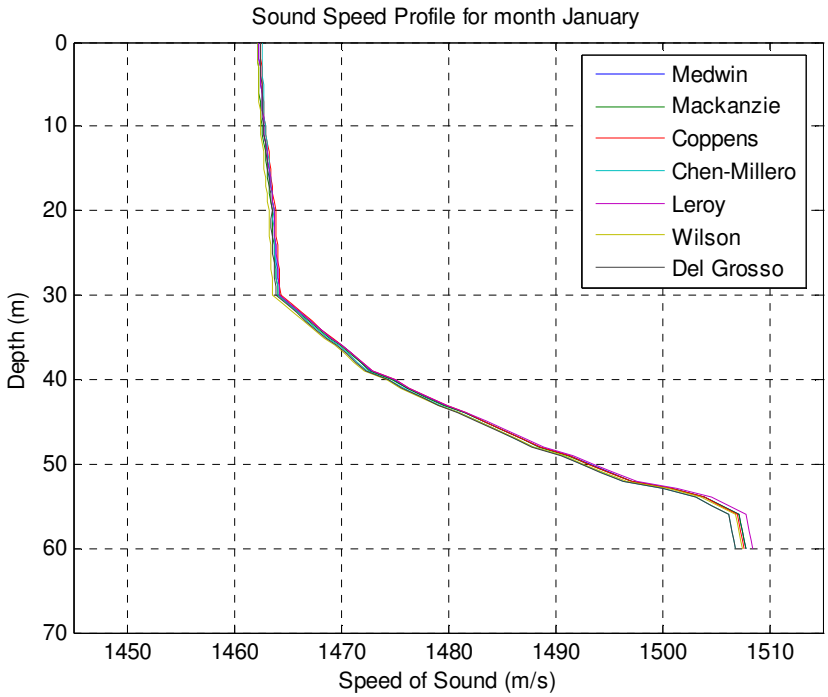

Figure 3.3: Sound speed profile calculated with different empirical formulas for the month of January 2005-2006.

As seen from the figure, although the validity ranges of the formulas are different, the results are very close.

4. SOUND PROPAGATION MODELS

Sound propagation in the broadest sense is described by the wave equation and the boundary conditions of the ocean environment. On the other hand, other simpler methods of modeling sound propagation in the sea are available. Basically, there are four different approaches: the ray theory, the spectral method or fast field program (FFP), the normal mode (NM) approach, and the parabolic equation (PE) approximation [1].

4.1 Wave Equation

Three-dimensional, time-dependent wave equation is the starting point of all the formulations of the acoustic propagation models:

$$\nabla^2 \Phi = \frac{1}{c^2} \frac{\partial^2 \Phi}{\partial t^2} \qquad \textbf{(4.1)}$$

where ∇^2 is the Laplacian operator $\left[= \left(\partial^2 / \partial x^2\right) + \left(\partial^2 / \partial y^2\right) + \left(\partial^2 / \partial z^2\right)\right]$, Φ is the potential function, c is the sound speed and t is the time.

The wave equation is usually converted to the Helmholtz equation which is a time-independent equation by assuming a harmonic (single-frequency, continuous wave) solution for the potential function Φ:

$$\Phi = \phi e^{-i\omega t} \qquad \textbf{(4.2)}$$

In the above equation, ϕ is a time-independent potential function and ω is the source frequency which is equal to $2\pi f$ [6]. If equation (4.2) is substituted into equation (4.1), the wave equation (4.1) becomes the elliptic Helmholtz equation in terms of the velocity potential ϕ:

$$\nabla^2\phi + k^2\phi = 0 \quad \textbf{(4.3)}$$

and in terms of the pressure p where $p = \rho i\omega\phi$ [6, 17]:

$$\nabla^2 p + k^2 p = 0 \quad \textbf{(4.4)}$$

Here, k indicates the wave number and is equal to $\omega / c = 2\pi / \lambda$ where λ is the wavelength [6].

In cylindrical co-ordinates equation (4.4) takes the form

$$\frac{\partial^2 p}{\partial r^2} + \frac{1}{r}\frac{\partial p}{\partial r} + \frac{\partial^2 p}{\partial z^2} + \frac{1}{r^2}\frac{\partial^2 p}{\partial \theta^2} + k^2 p = 0 \quad \textbf{(4.5)}$$

where r is the radial distance from the source, θ is the azimuthal angle on the horizontal $x - y$ plane, and z is the vertical distance. Between the Cartesian and cylindrical co-ordinates we have $x = r\cos\theta$, $y = r\sin\theta$ and $z = z$.

4.2 Acoustic Modeling Techniques

According to the theoretical approaches applied to the Helmholtz equation, acoustic propagation models can be classified into five main groups: 1) Ray theory, 2) Normal mode approach, 3) Multipath expansion, 4) Fast field approach, and 5) Parabolic equation techniques. These five main groups can also be sub-divided as range independent and range dependent types. If the ocean environment is assumed as cylindrically symmetric, which means it is horizontally stratified and its properties changes only with depth, the model is said to be range independent. On the other hand, in range dependent type, range (r) and azimuth (θ) variations are also considered. Range dependence can be thought as two-dimensional (2-D) or three-dimensional (3-D) according to the range and depth variations, or range, depth and azimuthal variations, respectively [6].

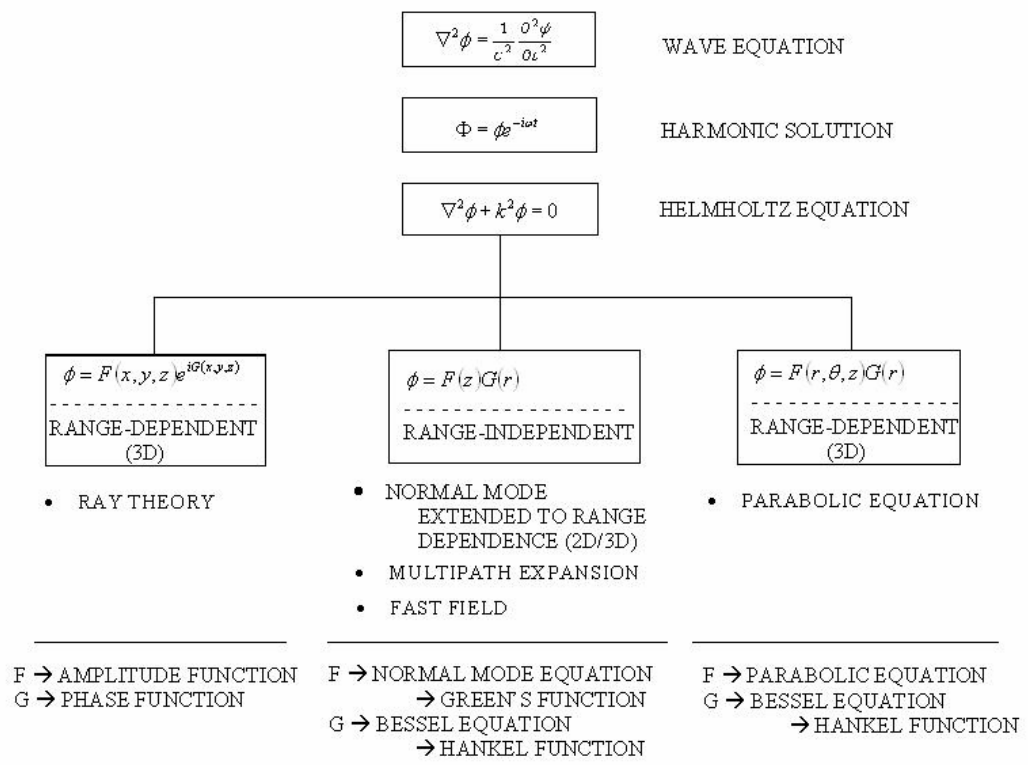

Figure 4.1: Classification of acoustic propagation models.

5. METHOD OF RAY TRACING

Ray tracing is the basis of ray-theoretical models [6]. It is an approximation done in the condition of high frequency (small wavelength). It defines the direction of propagating sound originating from a source in the water column [2]. Ray tracing code can be considered as the skeleton of the acoustic field. But, it should be noted that, in order to obtain the pressure field and the transmission loss, a ray tracing code is not enough. Phase and amplitude with each ray is needed to obtain the pressure field. By solving the eikonal and transport equations, phase and amplitude are obtained respectively [1]. If these further points are left aside, ray tracing can be considered as a good tool to visualize the sound propagation [2].

5.1 Ray Tracing Computation

Starting point of ray tracing is the Helmholtz equation in Cartesian coordinates $\vec{x} = (x, y, z)$, which is:

$$\nabla^2 p + \frac{\omega^2}{c^2(\vec{x})} p = -\delta(\vec{x} - \vec{x}_s) \qquad \textbf{(5.1)}$$

where ∇^2 is the Laplacian, *c(x)* is the sound speed and ω is the angular frequency of the source located at x_s.

In order to obtain ray equations, a series expansion form, which is called ray series, is taken as a solution to the Helmholtz equation [18].

$$p(\vec{x}) = e^{i\omega\tau(\vec{x})} \sum_{j=0}^{\infty} \frac{A_j(\vec{x})}{(i\omega)^j} \qquad \textbf{(5.2)}$$

First, the derivatives of ray series are

$$p_x = e^{i\omega\tau}\left[i\omega\tau_x \sum_{j=0}^{\infty} \frac{A_j}{(i\omega)^j} + \sum_{j=0}^{\infty} \frac{A_{j,x}}{(i\omega)^j} \right] \tag{5.3}$$

$$p_{xx} = e^{i\omega\tau}\left\{ \left[-\omega^2 (\tau_x)^2 + i\omega\tau_{xx} \right] \sum_{j=0}^{\infty} \frac{A_j}{(i\omega)^j} + 2i\omega\tau_x \sum_{j=0}^{\infty} \frac{A_{j,x}}{(i\omega)^j} + \sum_{j=0}^{\infty} \frac{A_{j,xx}}{(i\omega)^j} \right\} \tag{5.4a}$$

Equation (5.4a) can also be written as

$$\nabla^2 p = e^{i\omega\tau}\left\{ \left[-\omega^2 |\nabla\tau|^2 + i\omega\nabla^2\tau \right] \sum_{j=0}^{\infty} \frac{A_j}{(i\omega)^j} + 2i\omega\nabla\tau \sum_{j=0}^{\infty} \frac{\nabla A_j}{(i\omega)^j} + \sum_{j=0}^{\infty} \frac{\nabla^2 A_j}{(i\omega)^j} \right\} \tag{5.4b}$$

Then, substituting the above expressions into equation (5.1), and arranging the terms of order ω^2, the eikonal equation, which is a nonlinear partial differential equation, is obtained:

$$\left|\vec{\nabla}\tau\right|^2 = \frac{1}{c^2(\vec{x})} \tag{5.5}$$

Eikonal equation is used to obtain the ray paths of propagating sound. As seen in the figure 5.1, a wave front is defined by the level curves $\tau(\vec{x})$, and the rays are the normals to these wave fronts.

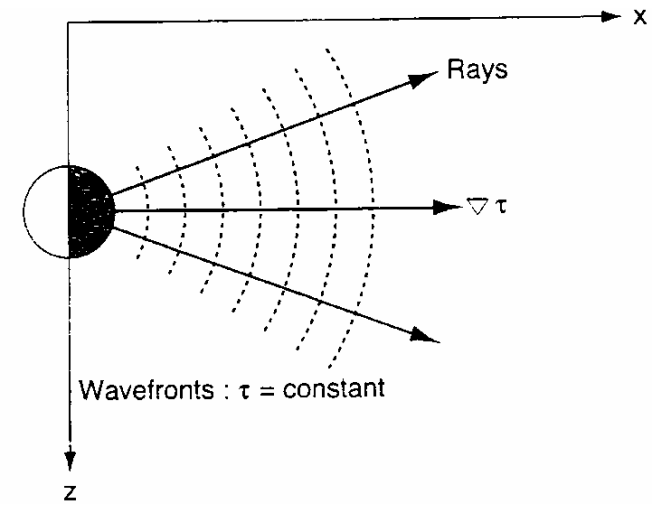

Figure 5.1: Rays and wavefronts.

From the figure, ray trajectory $\vec{x}(s)$ can be expressed as;

$$\frac{d\vec{x}}{ds} = c\vec{\nabla}\tau \tag{5.6}$$

where $\vec{\nabla}\tau$ is a vector perpendicular to the wave fronts, and c is a factor used to ensure that the tangent vector $d\vec{x}/ds$ has unit length. In order to verify the quantity of $d\vec{x}/ds$, the square of the equation (5.6) is taken and

$$\left|\frac{d\vec{x}}{ds}\right|^2 = c^2\left|\vec{\nabla}\tau\right|^2$$

is obtained. Here, the right hand side of the equation is found to be unity from the eikonal equation (5.5). Now, s is seen as the arc length along the ray because of the $|d\vec{x}/ds| = 1$ equality. Because $\tau(x)$ is an unknown function, we begin with differentiating equation (5.6) with respect to s and then substituting the eikonal equation into it, so that ray equation which involves only $c(\boldsymbol{x})$ is obtained.

$$\frac{d}{ds}\left(\frac{1}{c}\frac{d\vec{x}}{ds}\right) = -\frac{1}{c^2}\vec{\nabla}c \tag{5.7}$$

The above equation can be expressed in cylindrical coordinates (r,θ,z) where for simplicity, it is thought to be cylindrically symmetric. That is to say, there is no dependence to the azimuthal angle θ in the range-depth plane:

$$\frac{dr}{ds} = c\xi(s) \tag{5.8a}$$

$$\frac{d\xi}{ds} = -\frac{1}{c^2}\frac{dc}{dr} \tag{5.8b}$$

$$\frac{dz}{ds} = c\zeta(s) \tag{5.9a}$$

$$\frac{d\zeta}{ds} = -\frac{1}{c^2}\frac{dc}{dz} \tag{5.9b}$$

Note that by using the auxiliary variables $\xi(s)$ and $\zeta(s)$, equation (5.7) is written in the first-order form. Here, [*r(s), z(s)*] is the trajectory of the ray in the range-depth plane; [*dr/ds, dz/ds*] is the tangent vector to a curve, and $c[\,\xi(s), \zeta(s)\,]$ is the tangent vector to the ray.

In order to solve these first-order ordinary differential equations, the boundary condition which is the source position of the ray (r_s, z_s) with a specified take-off angle θ, is also needed and is expressed by

$$r = r_s \quad , \qquad \xi = \frac{\cos\theta}{c(0)} \tag{5.10}$$

$$z = z_s \quad , \qquad \zeta = \frac{\sin\theta}{c(0)} \tag{5.11}$$

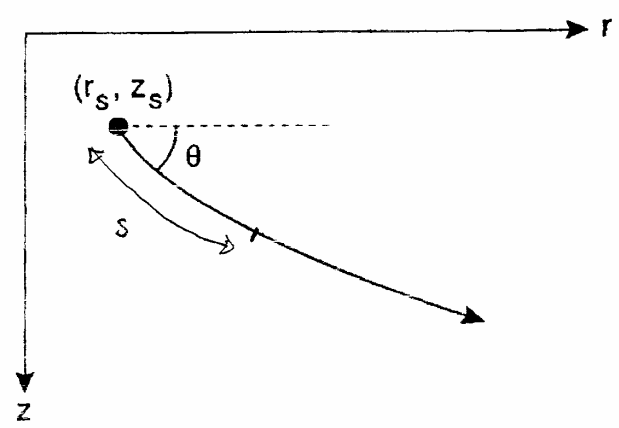

Figure 5.2: Boundary condition shown in 2-D geometry.

5.2 Alternative Ray Tracing Computation

Ray tracing equations can also be expressed by canceling out *ds*. In order to to this, equation (5.8b), (5.9a), (5.9b) are divided by the equation (5.8a), so that

$$\frac{dz}{dr} = \frac{\zeta}{\xi} \tag{5.12}$$

$$\frac{d\xi}{dr} = -\frac{c_r}{c^3 \xi} \tag{5.13}$$

$$\frac{d\zeta}{dr} = -\frac{c_z}{c^3 \xi} \tag{5.14}$$

Differentiating equation (5.12) with respect to *r*, and substituting (5.13) and (5.14) into it, gives

$$\frac{d^2 z}{dr^2} = \frac{-c_z + \left(\zeta \big/ \xi\right) c_r}{\xi^2 c^3} \tag{5.15}$$

Rearranging equation (5.8a) and taking the square of it, we obtain

$$\xi^2 = \frac{1}{c^2}\left(\frac{dr}{ds}\right)^2 = \frac{1}{c^2}\frac{(dr)^2}{(dr)^2 + (dz)^2} = \frac{1}{c^2}\frac{1}{1 + \left(dz \big/ dr\right)^2} \tag{5.16}$$

which in turn is used in (5.15) to get

$$\frac{d^2 z}{dr^2} = \left[1 + \left(\frac{dz}{dr}\right)^2\right]\left[-\frac{c_z}{c} + \underbrace{\left(\frac{dz}{dr}\right)\frac{c_r}{c}}_{ignore}\right] = \left[1 + \left(\frac{dz}{dr}\right)^2\right]\left[-\frac{c_z}{c}\right] \tag{5.17}$$

which may be conveniently used in a ray tracing computer code. The boundary conditions of this ray tracing are, $z(0) = z_{source}$ and $\left.\frac{\partial z}{\partial r}\right|_{r=0} = \tan\theta_0$, which represent the starting point of the rays at the source depth and launch angle θ_0 of a given ray, respectively [1].

In the numerical implementation of ray tracing code, a source at depth 0 m and a receiver at depth 10 m are placed. The surface and the bottom are thought as walls with total reflection. For the case of the source at the surface, the launch angle is adjusted so that none of the sound waves can go out above the surface. Also, the condition is placed to see only the propagation paths within the 10 m above and below the receiver. The curves obtained from the sound speed profiles are fitted with the polynomials by using least squares method and used in the ray tracing code as a sound speed function. The code is run for sound profiles of all the data covering the twelve months. As an example, the results for the month of January are given below in Figures 5.3 and 5.4. The rest of the months are given in the appendix B. The results without the condition of 10m-above-and-below-the-receiver are also given in Appendix C.

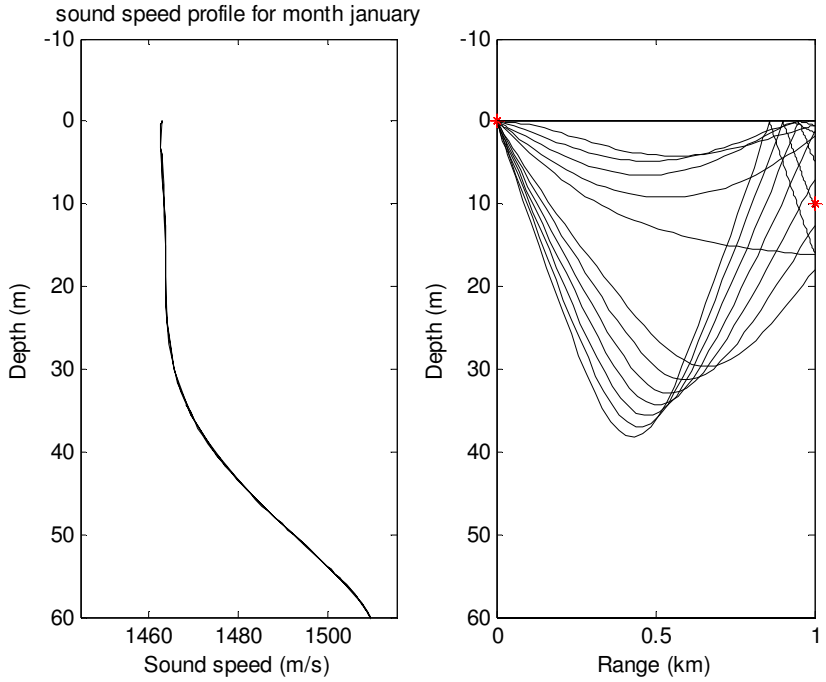

Figure 5.3: Result of ray tracing code for the month of January 2005-2006 with a condition of showing only the paths within the range of 10 m above and below the receiver.

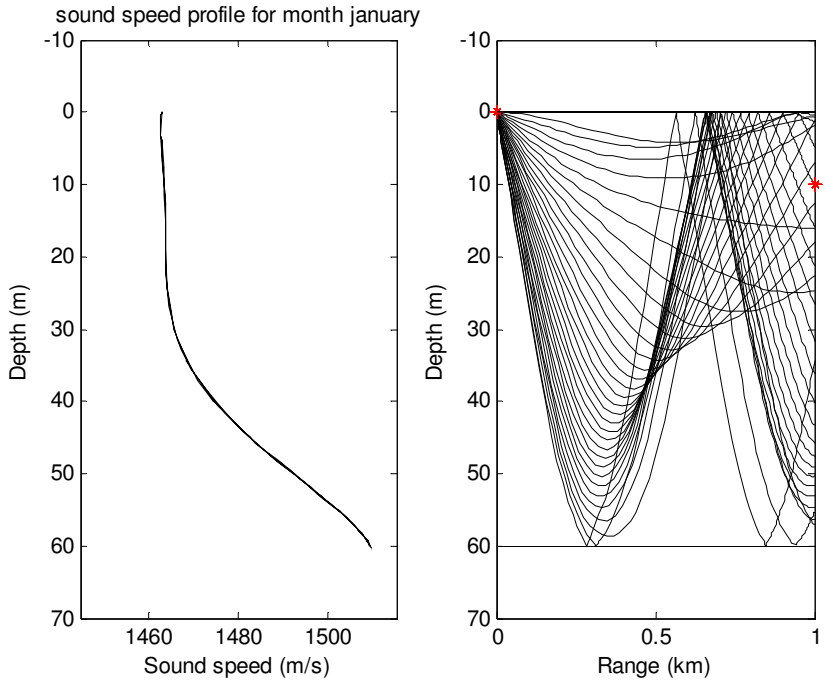

Figure 5.4: Result of ray tracing code for the month of January 2005-2006 without any condition about the receiver.

6. RESULTS AND DISCUSSION

In this study, one of the approaches of sound propagation models, ray theory, is applied to the real data with some restrictions. As mentioned before, ray tracing is the basis of ray theoretical models and can be considered as a good tool to visualize the sound propagation paths. It defines the direction of sound propagation originating from a source. However, it must be emphasized that ray tracing is an approximation done in the condition of high frequency. This means that the source must be a point source for not interfering with the waves emitted. In the ray tracing code, a point source and a point receiver are placed and the propagation paths are computed for all the available sound profiles covering twelve months. It is seen that as the sound speed profiles change for each month, propagation paths change accordingly. Here, only the skeleton of the acoustic field is shown. Pressure field and transmission loss is ignored because in order to obtain these, additional features are needed such as phase and amplitude values of each ray. This requires solving both the eikonal and transport equations derived from the wave equation. Here, only the eikonal equation is solved. For further study, both the eikonal and the transport equations can be solved. Also, the ray theory and other propagation models may be compared for sources and receivers placed at different depths and in different sea environment and bathymetries.

This is a basic study done in underwater acoustics; however, it should be indicated that there is no practical work using only ray tracing results. Rather, other methods must also be considered for a reliable description of the acoustic field. Nevertheless, ray tracing is a fundamental approach and may be used for exploring the basic acoustic characteristics of two-layer media.

REFERENCES

[1] **Kuperman, W.A., Roux, P.,** 2006. Introduction to Underwater Acoustics, Notes for a Short Course, October 2-6, 2006, Bodrum, Turkey

[2] http://staff.washington.edu/aganse/lunchtimesem.html

[3] http://solmar.nurc.nato.int/solmar/education/edu_sound_propagation.html

[4] http://freespace.virgin.net/mark.davidson3/reflection/reflection.html

[5] http://freespace.virgin.net/mark.davidson3/propagation/propagation.html

[6] **Etter, P.C.,** 1991. Underwater Acoustic Modeling: Principles, Techniques and Applications, Elsevier Science Publishers LTD, England.

[7] http://freespace.virgin.net/mark.davidson3/propagation/speed.html

[8] **Medwin, H.,** 1975. Speed of sound in water: A simple equation for realistic parameters, *J. Acoust. Soc. Am.,* **58(6),** 1318-1319.

[9] **Mackenzie, K.V.,** 1981. Nine-term equation for the sound speed in the oceans, *J. Acoust. Soc. Am.,* **70(3),** 807-812.

[10] **Coppens, A.B.,** 1981. Simple equations for the speed of sound in Neptunian waters, *J. Acoust. Soc. Am.,* **69(3),** 862-863.

[11] **Chen, C-T., Millero, F.J.,** 1977. Speed of sound in seawater at high pressures, *J. Acoust. Soc. Am.,* **62(5),** 1129-1135.

[12] **Leroy, C.C., Parthiot, F.,** 1998. Depth-pressure relationship in the oceans and seas, *J. Acoust. Soc. Am.,* **103(3),** 1346-1352.

[13] **Leroy, C.C.,** 1969. Development of Simple Equations for Accurate and More Realistic Calculation of the Speed of Sound in Seawater, *J. Acoust. Soc. Am.,* **46(1),** 216-226.

[14] **Wilson, W.D.,** 1960. Equation for the Speed of Sound in Sea Water, *J. Acoust. Soc. Am.,* **32(10),** 1357.

[15] **Del Grosso, V.A.,** 1974. New equation for the speed of sound in natural waters (with comparisons to other equations), *J. Acoust. Soc. Am.,* **56(4),** 1084-1091.

[16] National Physical Laboratory, Technical Guides, 2000, Middlesex, UK.

[17] http://scholar.lib.vt.edu/theses/available/etd-040799-41510/unrestricted/appa.pdf

[18] **Jensen, F.B. et al.,** 1994. Computational Ocean Acoustics, AIP Press, NY.

APPENDIX A

Sound Speed Profiles

Sound speed profiles generated by using empirical formulas for twelve months from January to December in the years of 2005-2006.

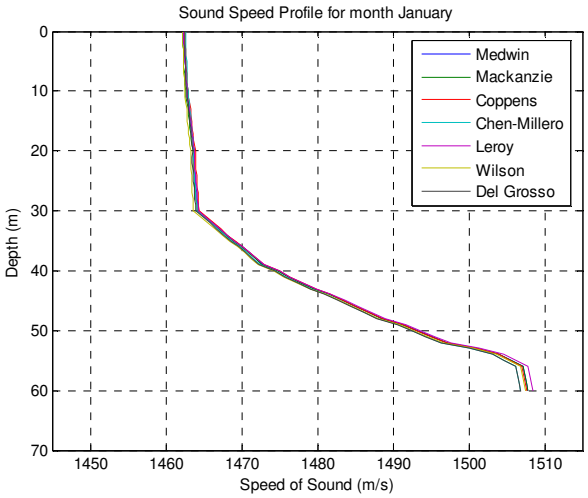

Figure A.1: Sound speed profile for the month of January.

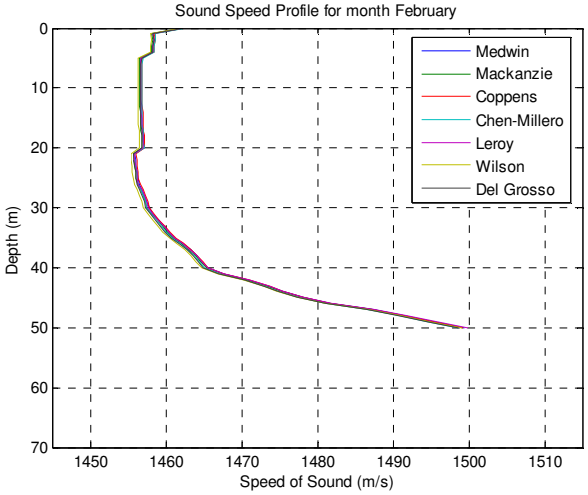

Figure A.2: Sound speed profile for the month of February.

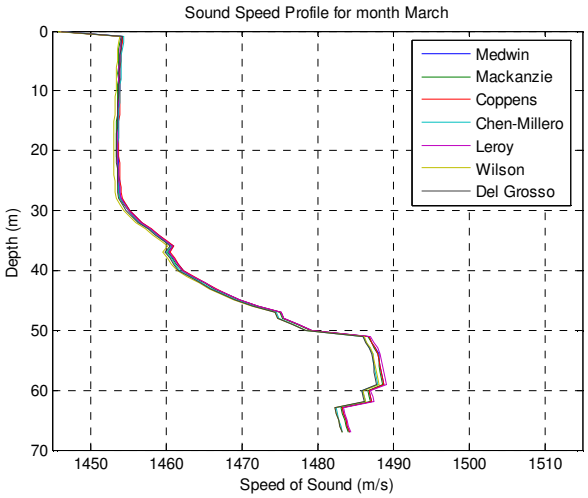

Figure A.3: Sound speed profile for the month of March.

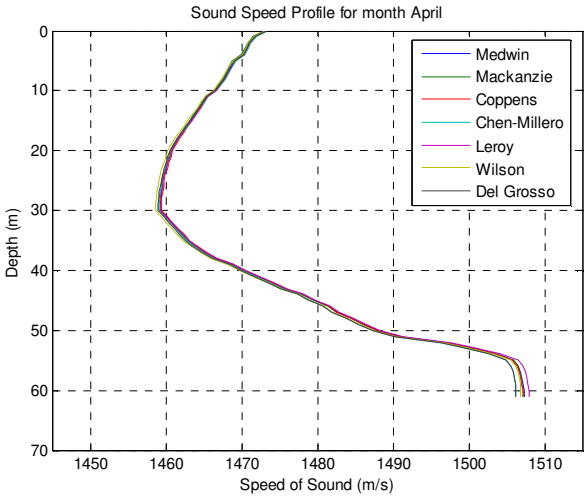

Figure A.4: Sound speed profile for the month of April.

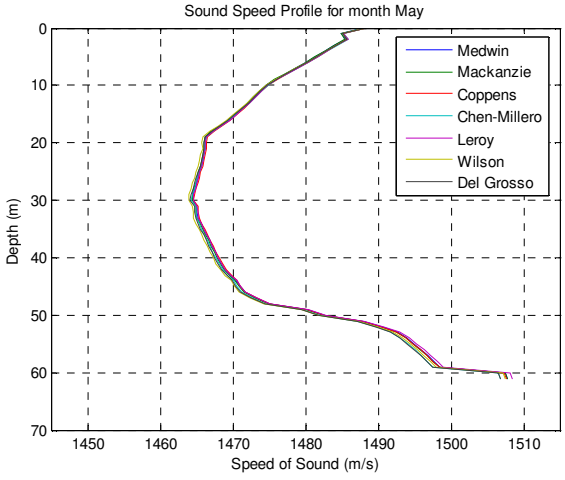

Figure A.5: Sound speed profile for the month of May.

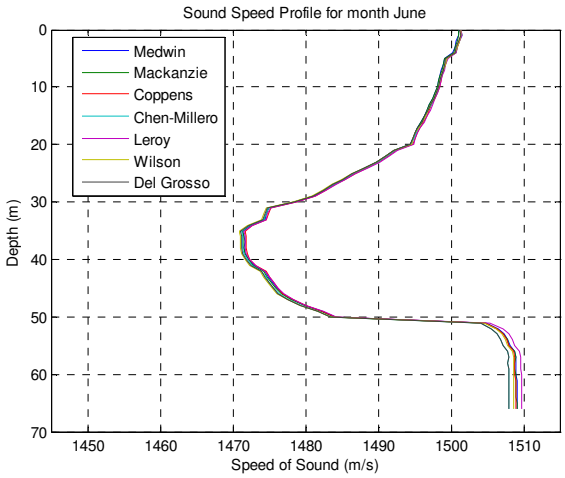

Figure A.6: Sound speed profile for the month of June.

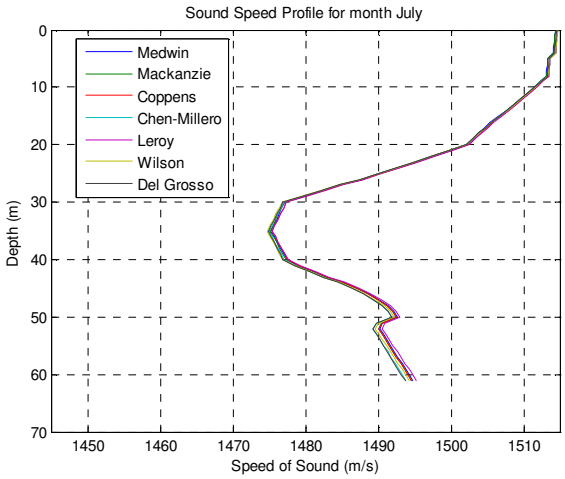

Figure A.7: Sound speed profile for the month of July.

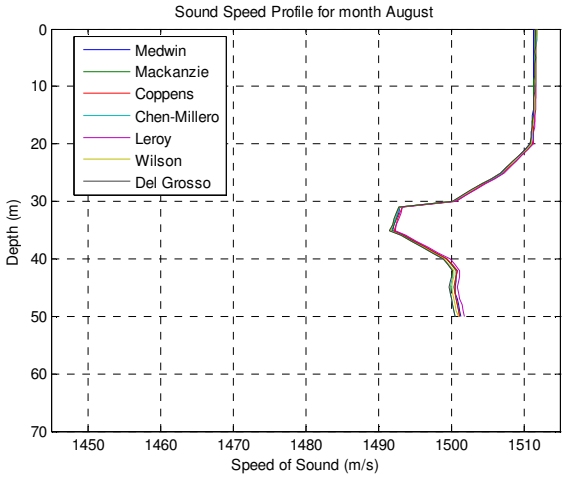

Figure A.8: Sound speed profile for the month of August.

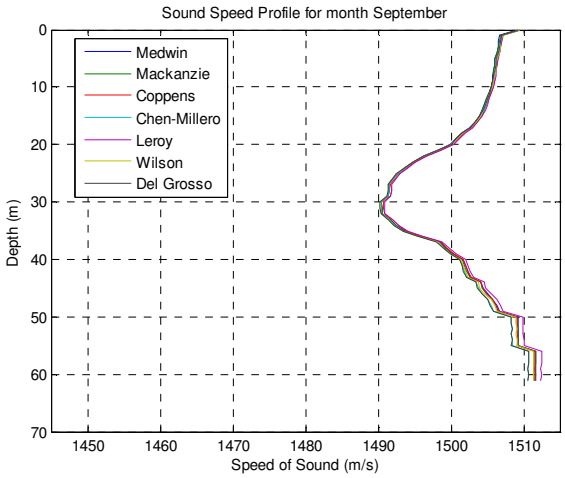

Figure A.9: Sound speed profile for the month of September.

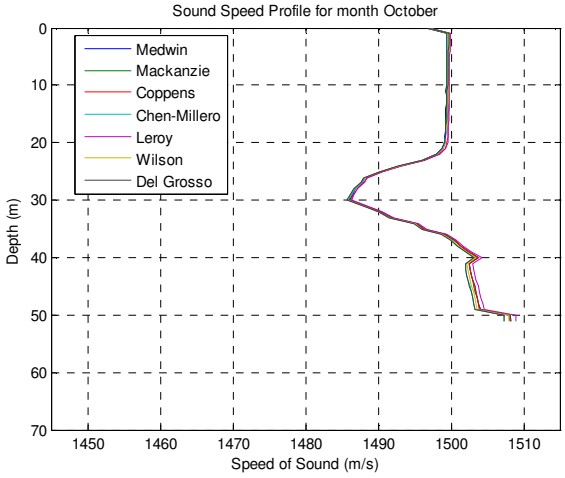

Figure A.10: Sound speed profile for the month of October.

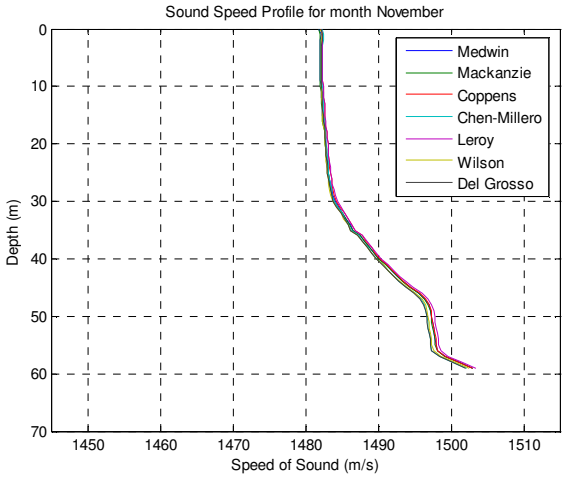

Figure A.11: Sound speed profile for the month of November.

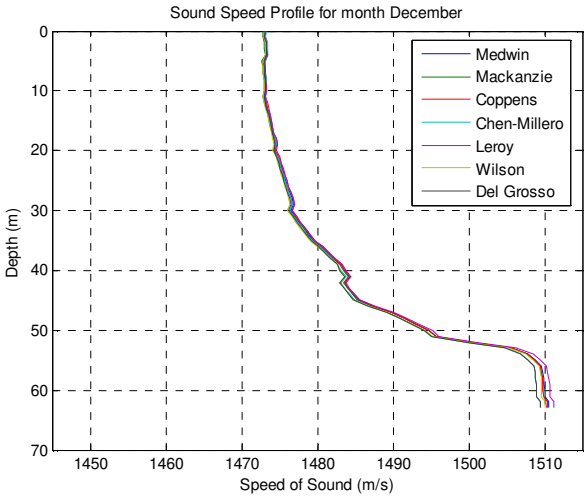

Figure A.12: Sound speed profile for the month of December.

APPENDIX B

Sound Propagation Paths

In this section sound speed profiles (ssp) and corresponding sound propagation paths are shown with the ray tracing code results. For the curve fitting of ssp of the months of January, February, March, April, May, September, November and December, sixth degree polynomials are used and for the months of June and July tenth degree polynomials are used. For the months of August and October, the data are divided into two parts for better curve fitting, and for the month of August and October, third degree polynomials are used for the first parts and a sixth degree polynomial and a fifth degree polynomial are used for the second part, respectively. In the code, a restriction may be imposed regarding the receiver position. Only the propagation paths within the 10 m above and below the receiver are shown. Figures without any range restrictions are given in appendix C.

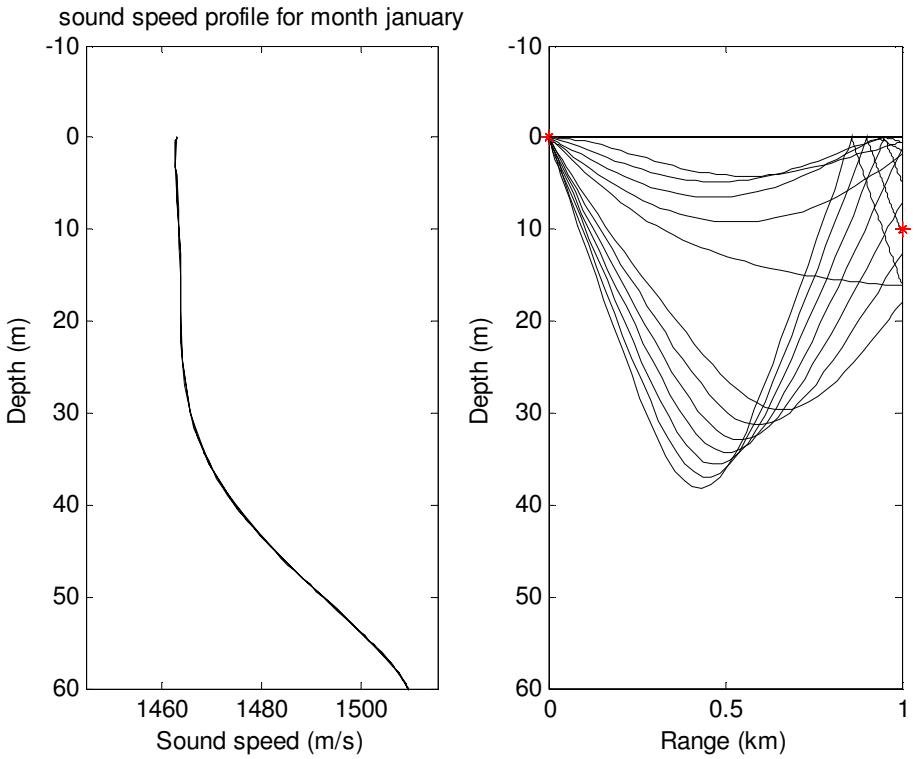

Figure B.1: Ssp and corresponding sound propagation paths for the month of January in the condition of 0 to 15° launch angle with 0.5° step.

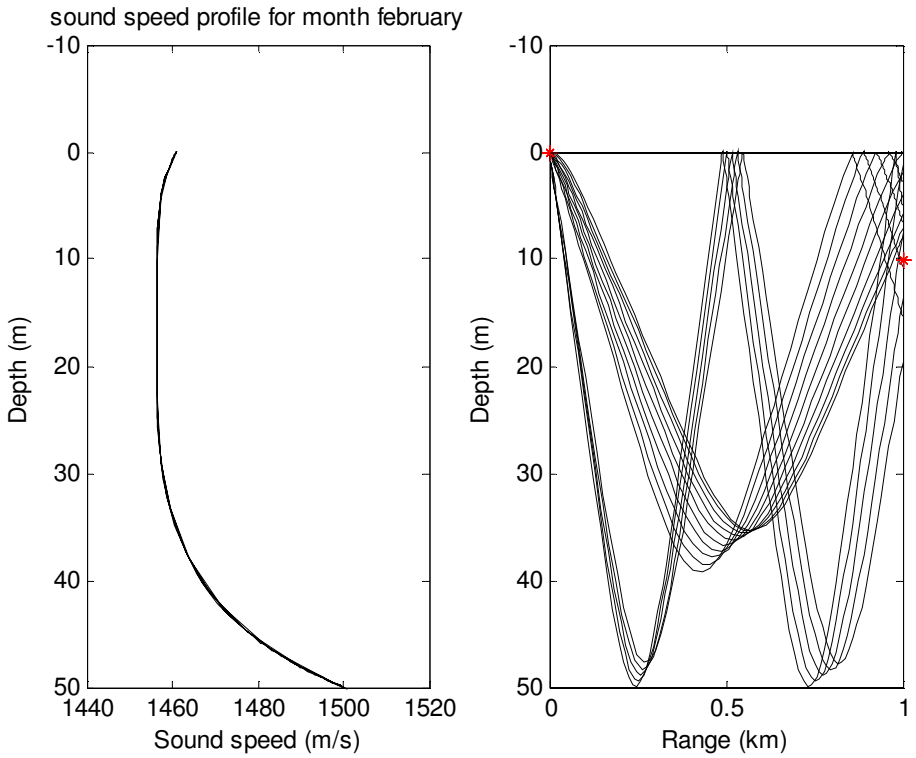

Figure B.2: Ssp and corresponding sound propagation paths for the month of February in the condition of 0 to 15° launch angle with 0.5° step.

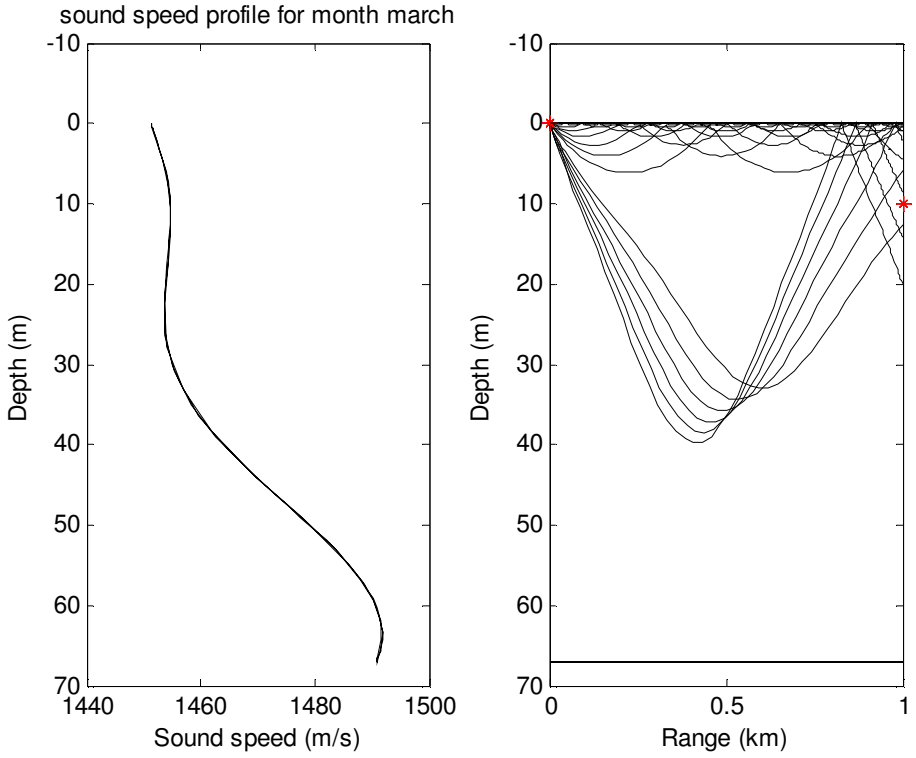

Figure B.3: Ssp and corresponding sound propagation paths for the month of March in the condition of 0 to 15° launch angle with 0.5° step.

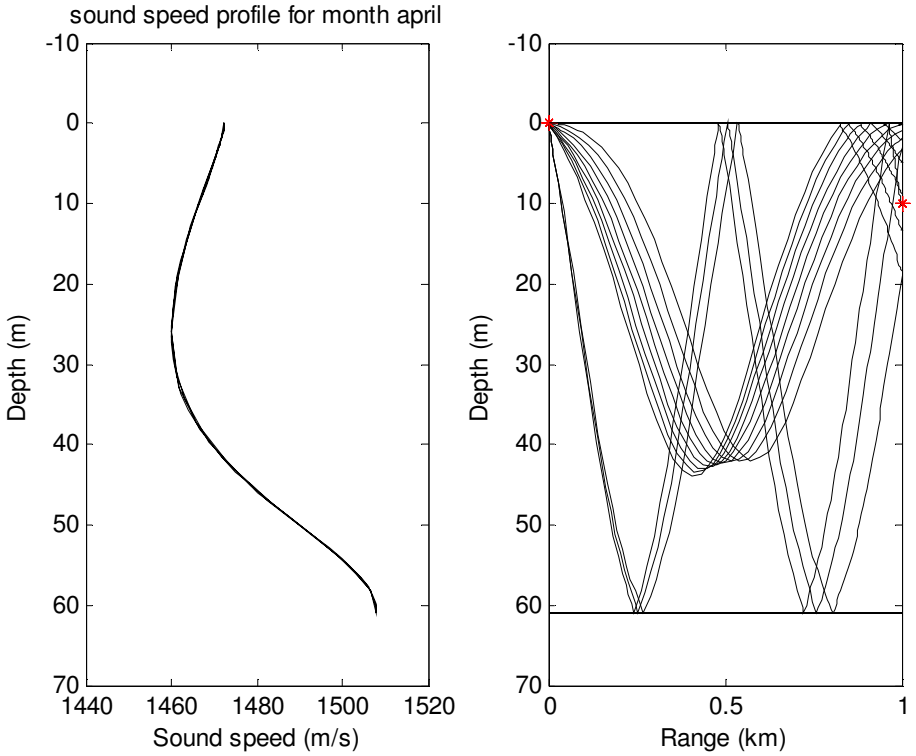

Figure B.4: Ssp and corresponding sound propagation paths for the month of April in the condition of 0 to 15° launch angle with 0.5° step.

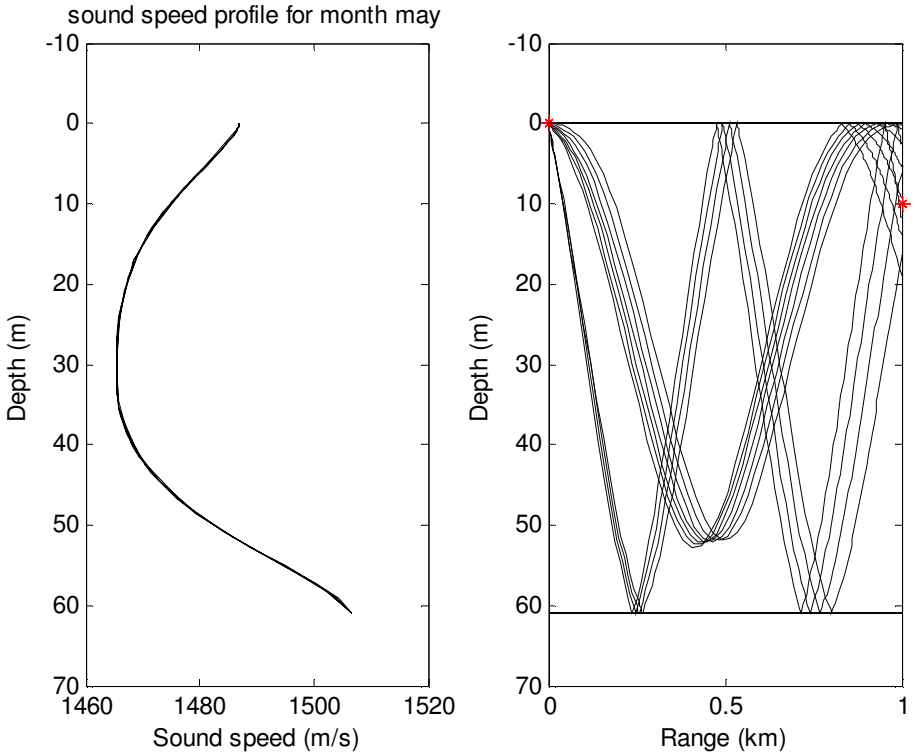

Figure B.5: Ssp and corresponding sound propagation paths for the month of May in the condition of 0 to 15° launch angle with 0.5° step.

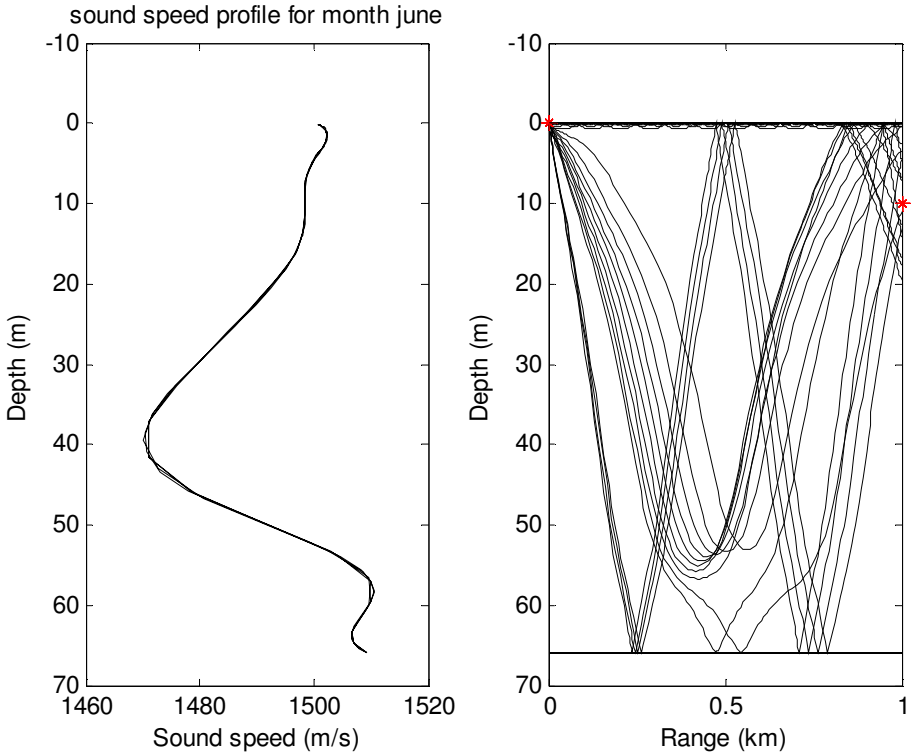

Figure B.6: Ssp and corresponding sound propagation paths for the month of June in the condition of 0.001 to 15° launch angle with 0.5° step.

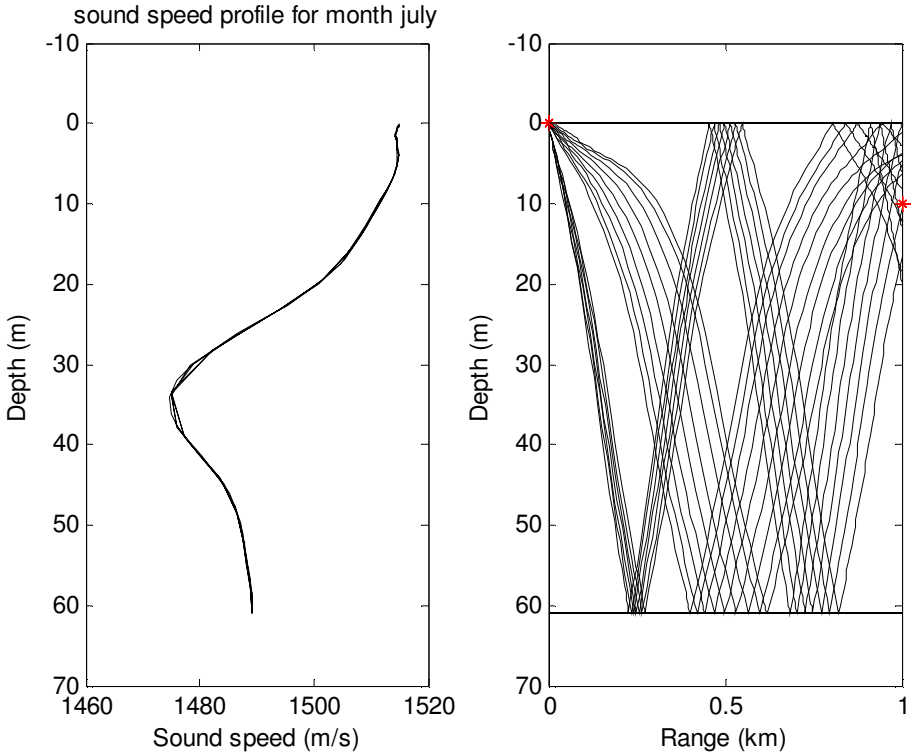

Figure B.7: Ssp and corresponding sound propagation paths for the month of July in the condition of 0 to 15° launch angle with 0.5° step.

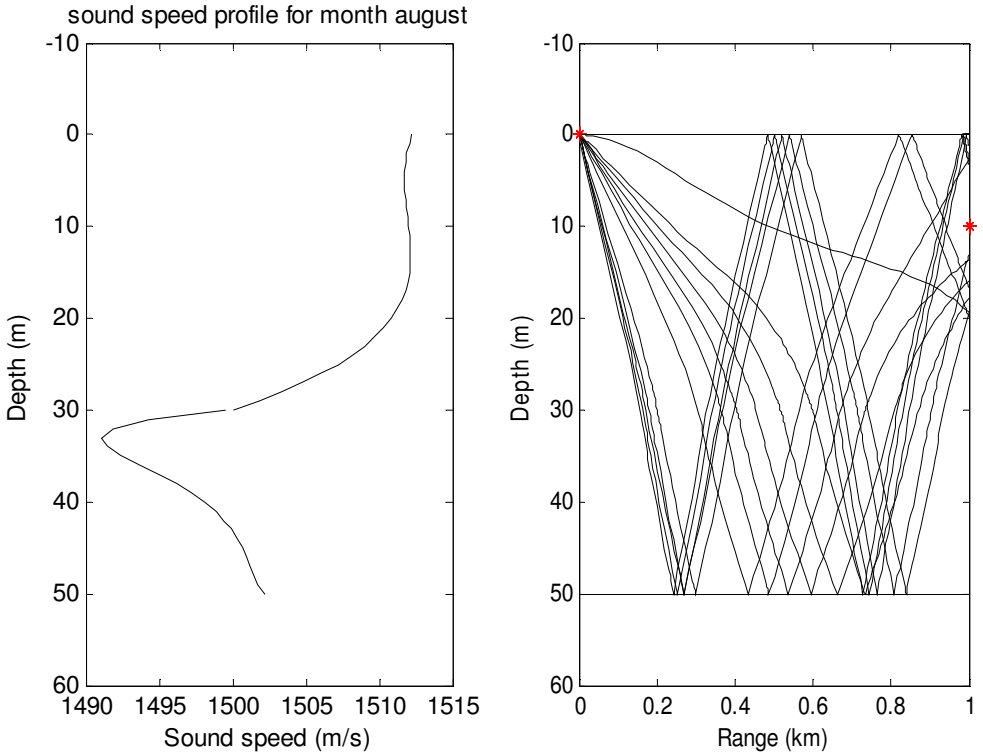

Figure B.8: Ssp and corresponding sound propagation paths for the month of August in the condition of 0 to 15° launch angle with 0.5° step.

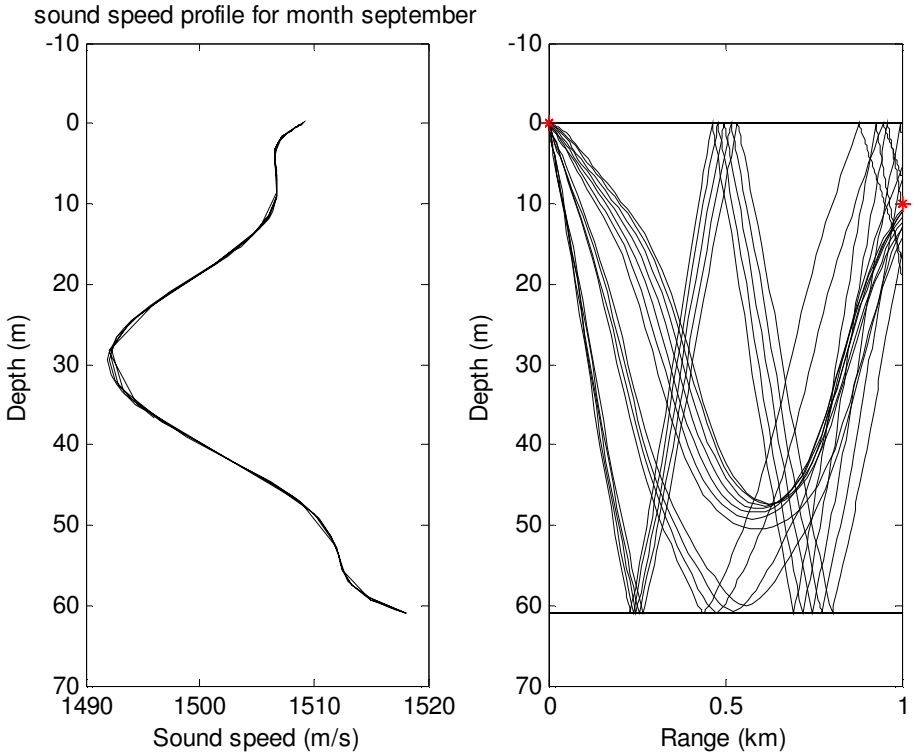

Figure B.9: Ssp and corresponding sound propagation paths for the month of September in the condition of 0 to 15° launch angle with 0.5° step.

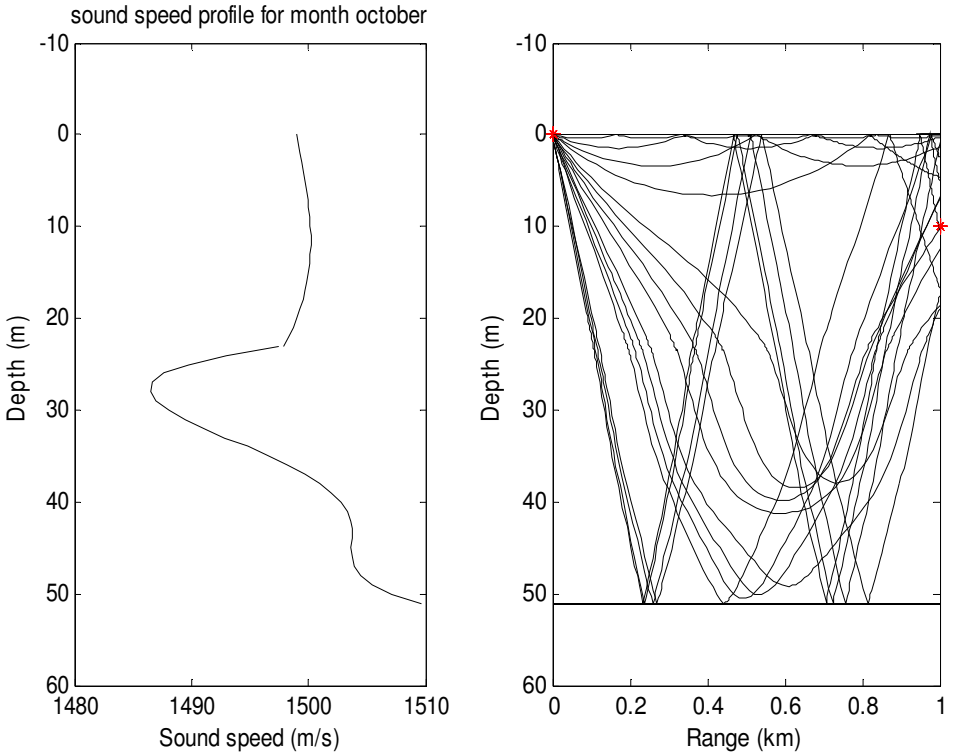

Figure B.10: Ssp and corresponding sound propagation paths for the month of October in the condition of 0 to 15° launch angle with 0.5° step.

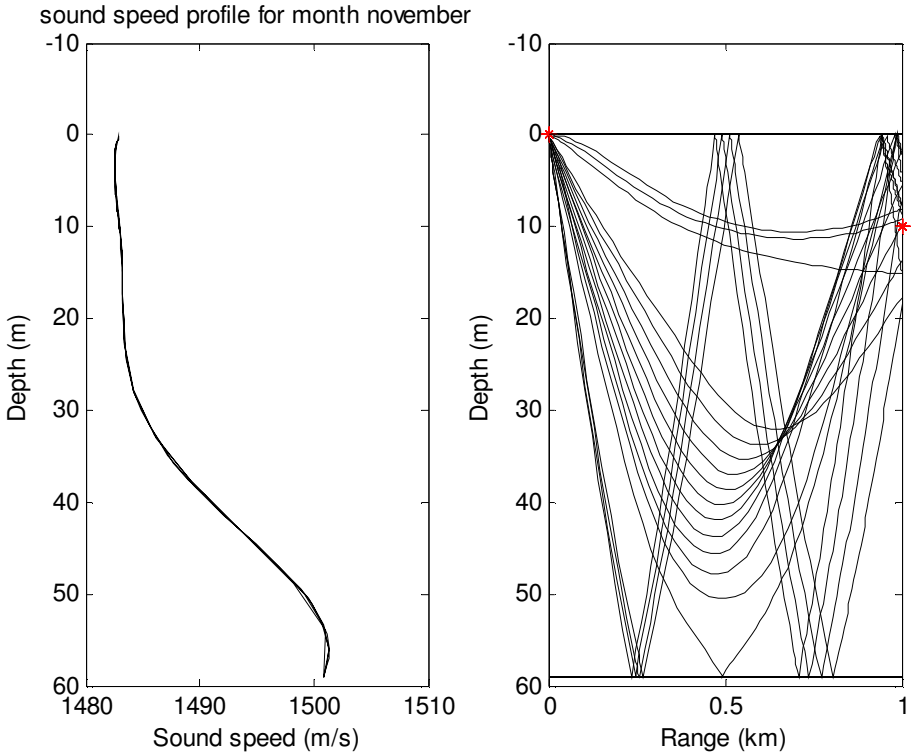

Figure B.11: Ssp and corresponding sound propagation paths for the month of November in the condition of 0 to 15° launch angle with 0.5° step.

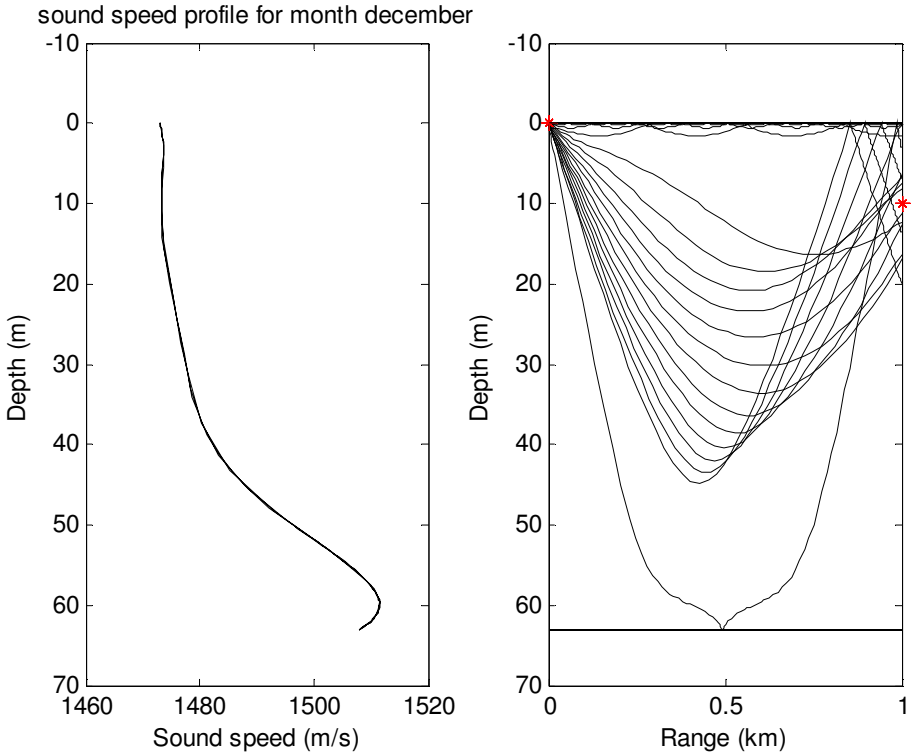

Figure B.12: Ssp and corresponding sound propagation paths for the month of December in the condition of 0.01 to 15° launch angle with 0.5° step.

APPENDIX C

Sound Propagation Paths without Any Limitation

In this section, sound propagation paths are given without any restriction on the receiver location as mentioned in appendix B.

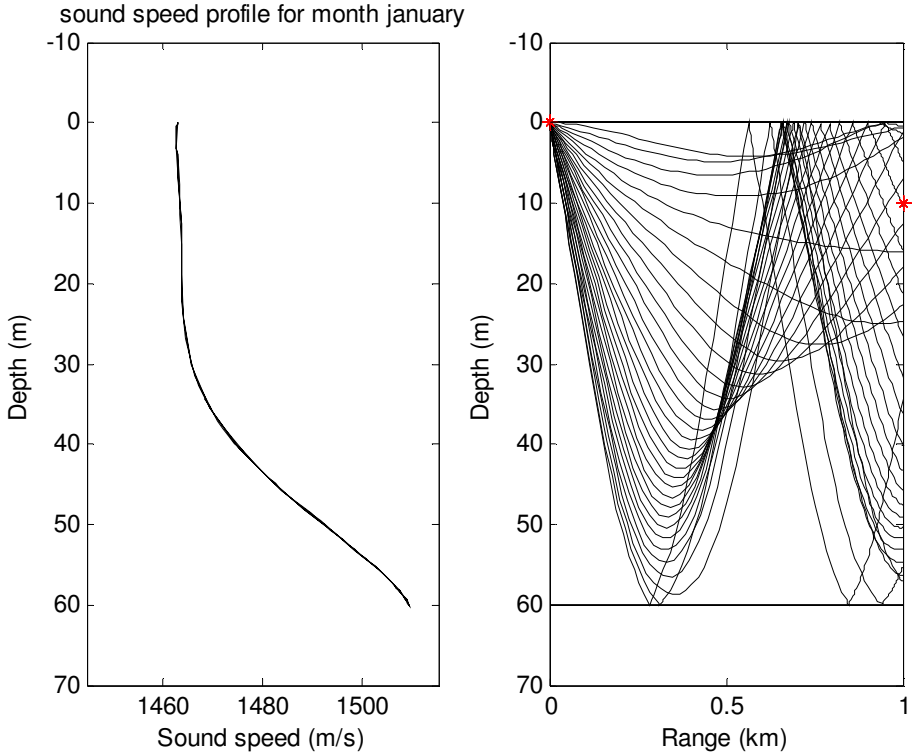

Figure C.1: Ssp and corresponding sound propagation paths for the month of January in the condition of 0 to 15° launch angle with 0.5° step.

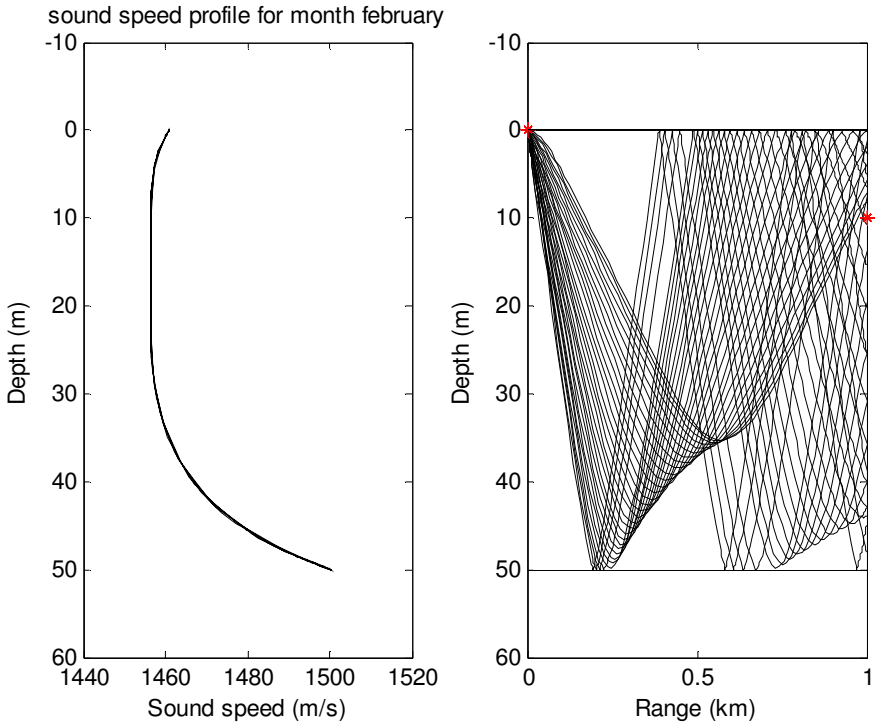

Figure C.2: Ssp and corresponding sound propagation paths for the month of February in the condition of 0 to 15° launch angle with 0.5° step.

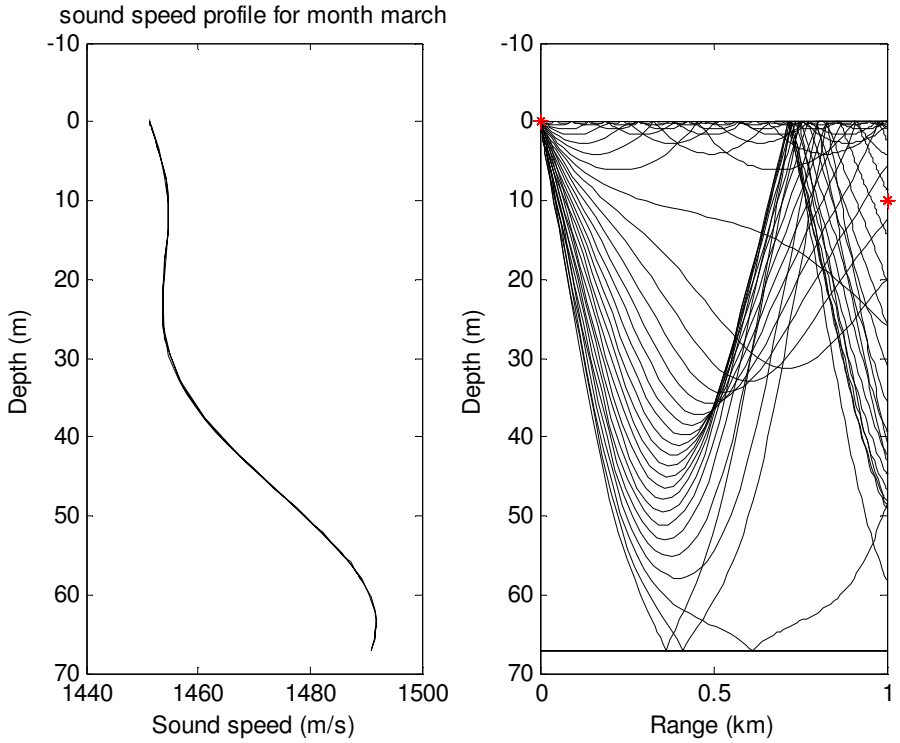

Figure C.3: Ssp and corresponding sound propagation paths for the month of March in the condition of 0 to 15° launch angle with 0.5° step.

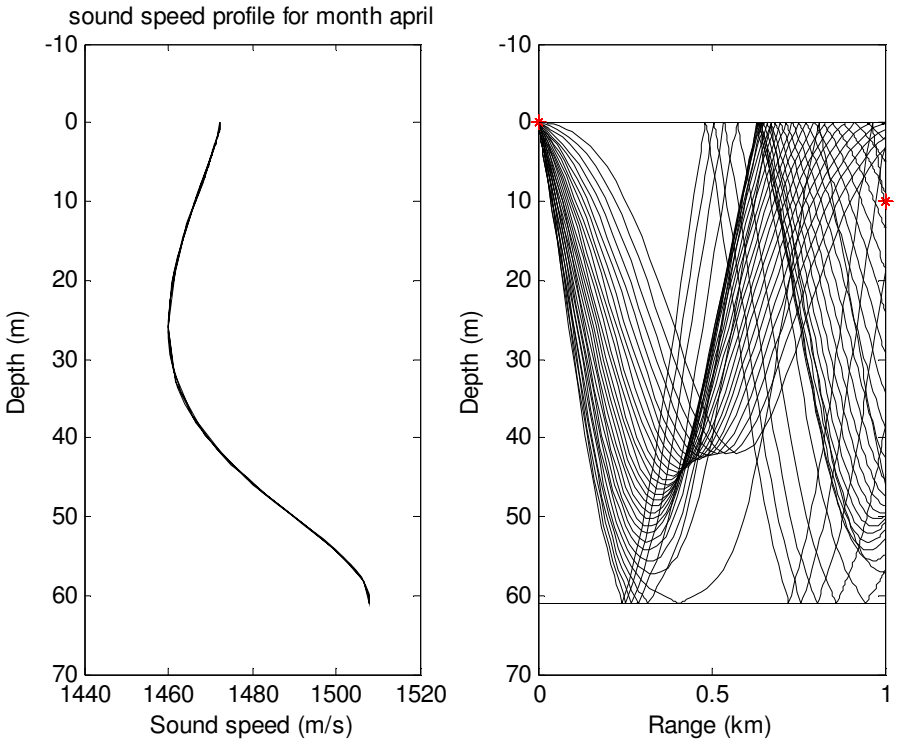

Figure C.4: Ssp and corresponding sound propagation paths for the month of April in the condition of 0 to 15° launch angle with 0.5° step.

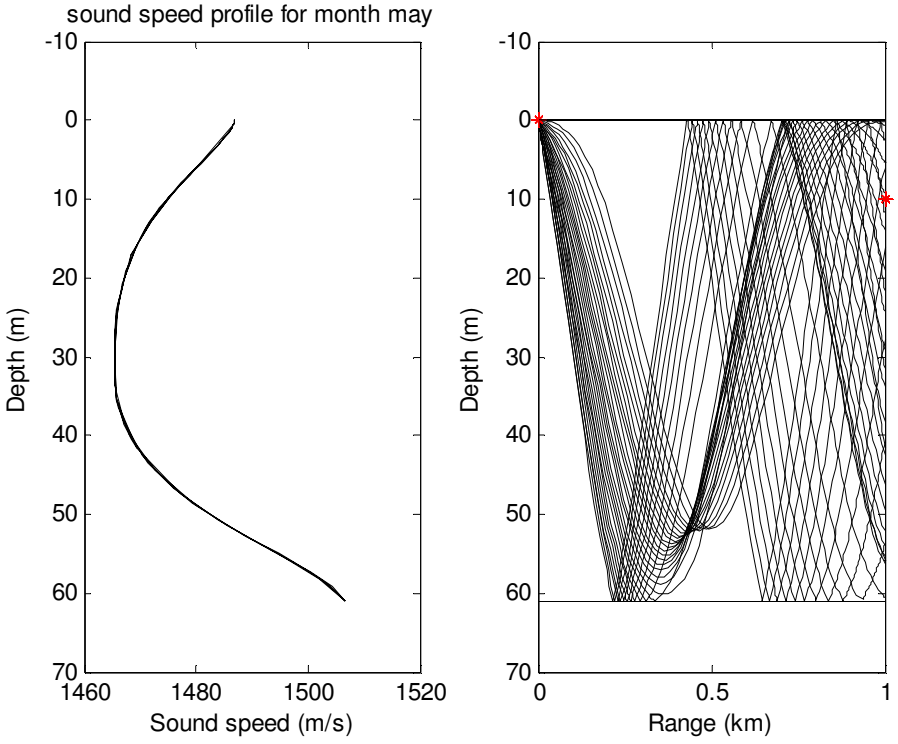

Figure C.5: Ssp and corresponding sound propagation paths for the month of May in the condition of 0 to 15° launch angle with 0.5° step.

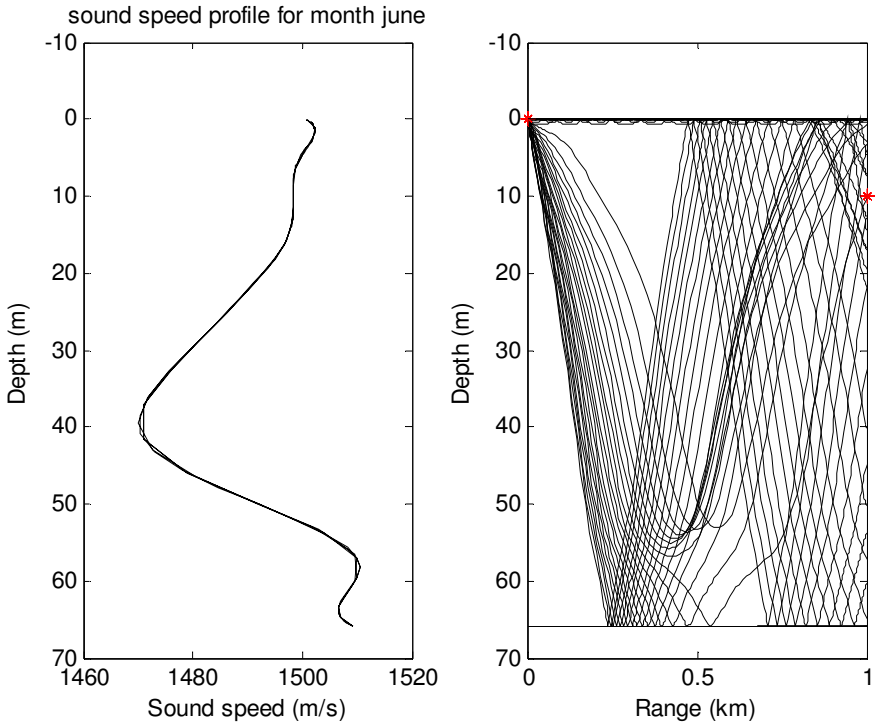

Figure C.6: Ssp and corresponding sound propagation paths for the month of June in the condition of 0.001 to 15° launch angle with 0.5° step.

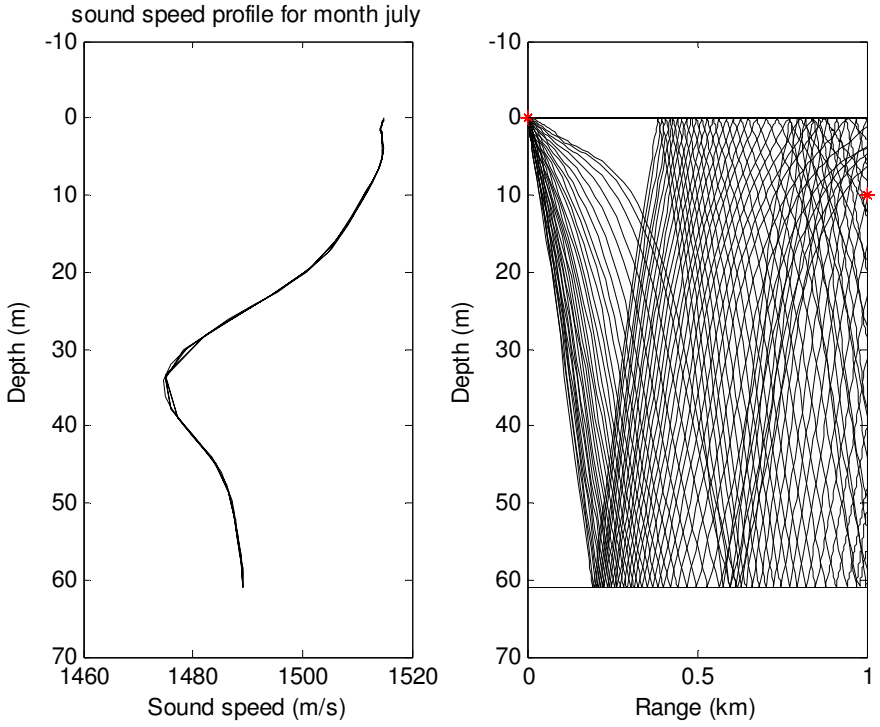

Figure C.7: Ssp and corresponding sound propagation paths for the month of July in the condition of 0 to 15° launch angle with 0.5° step.

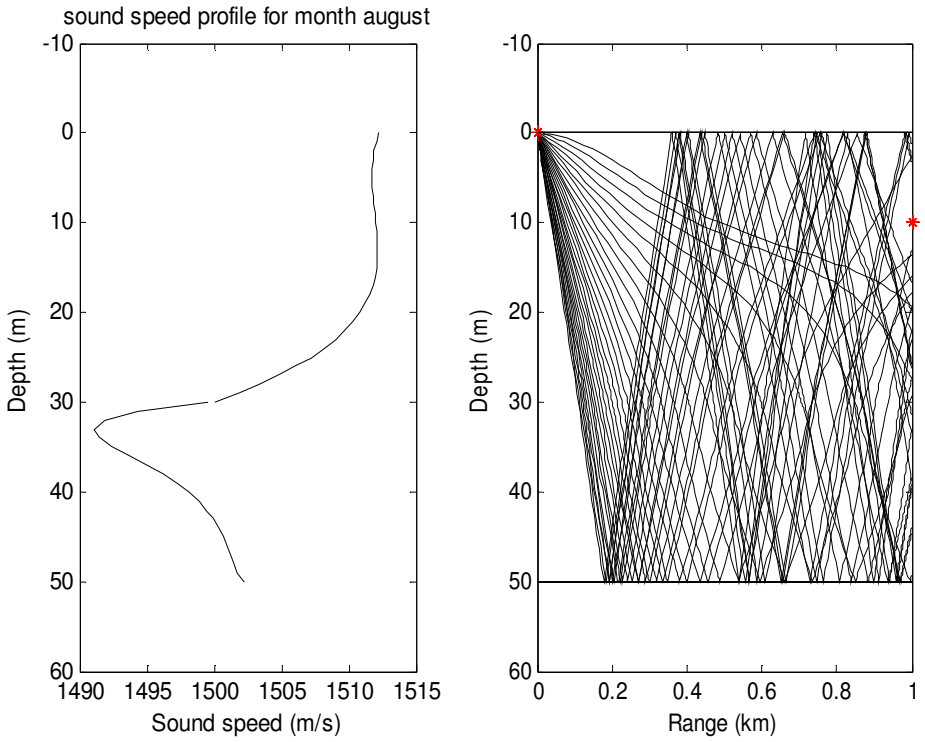

Figure C.8: Ssp and corresponding sound propagation paths for the month of August in the condition of 0 to 15° launch angle with 0.5° step.

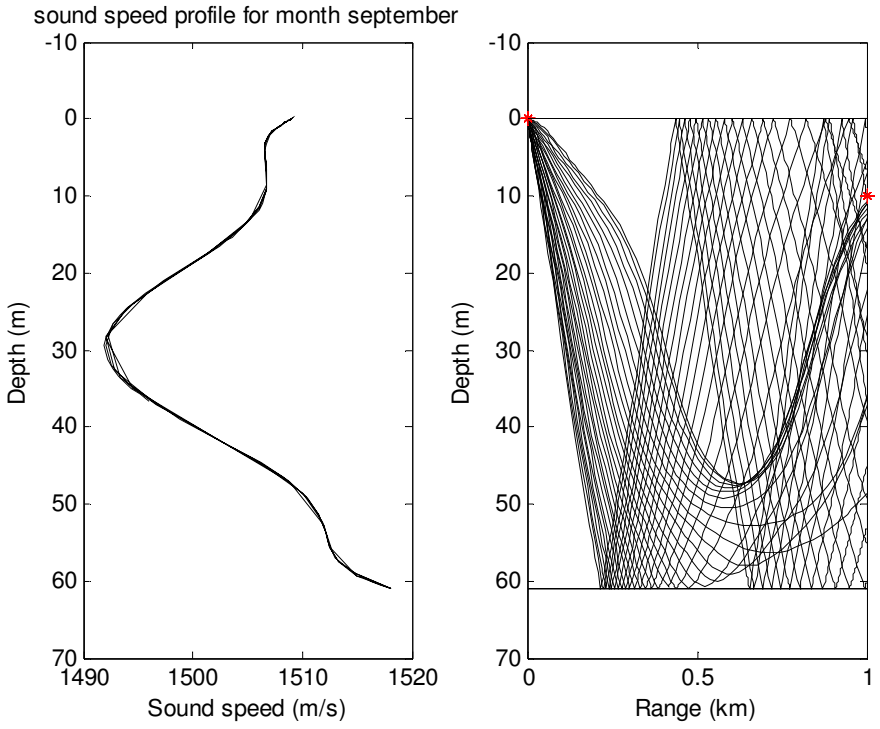

Figure C.9: Ssp and corresponding sound propagation paths for the month of September in the condition of 0 to 15° launch angle with 0.5° step.

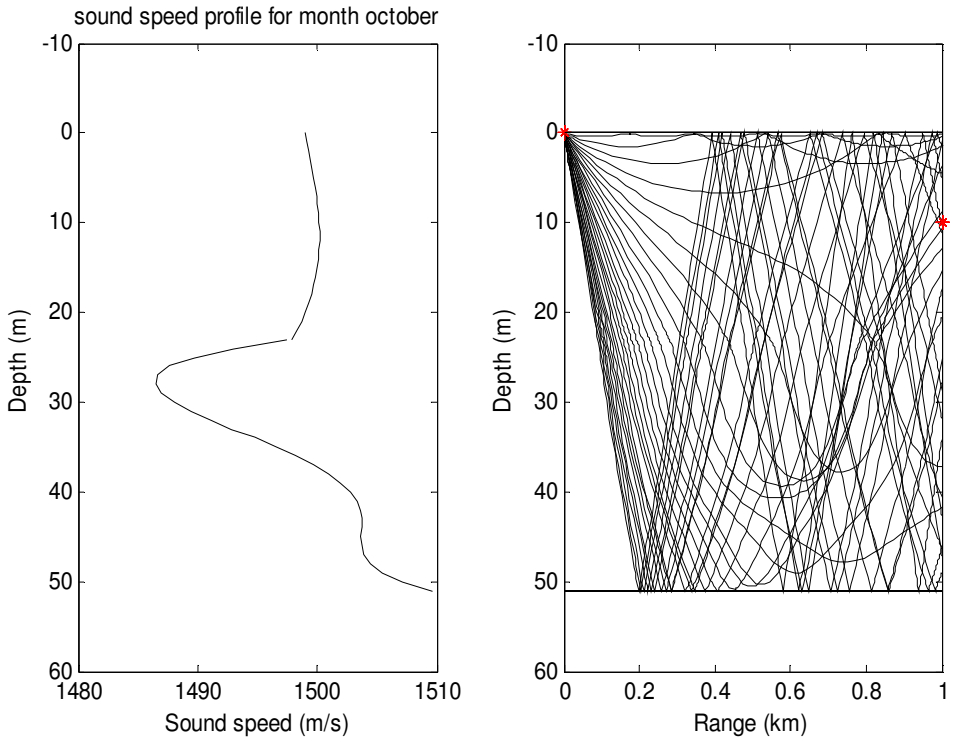

Figure C.10: Ssp and corresponding sound propagation paths for the month of October in the condition of 0.01 to 15° launch angle with 0.5° step.

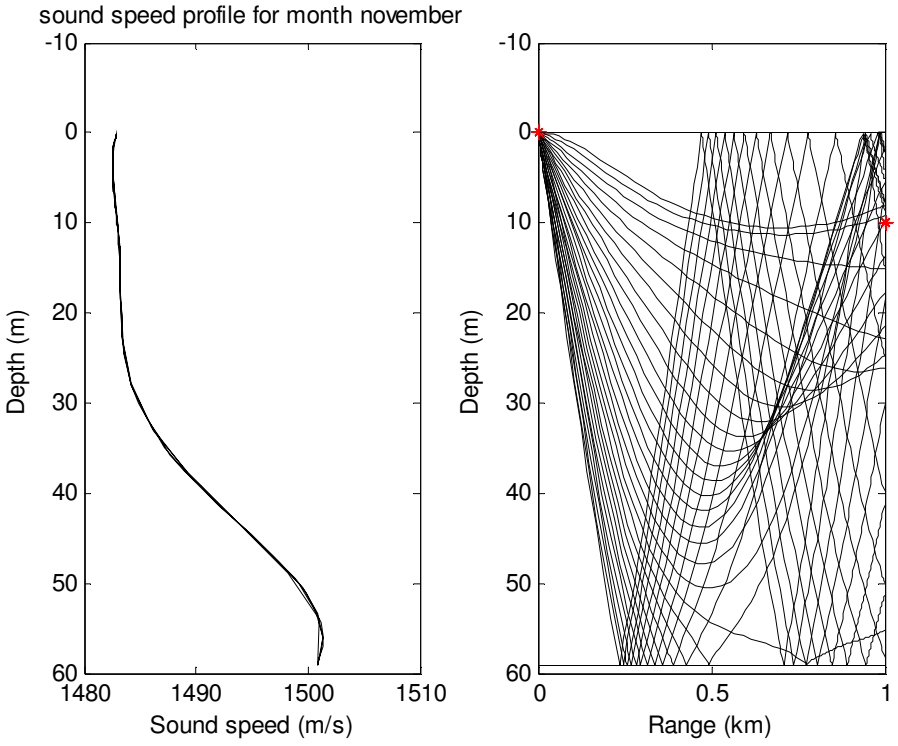

Figure C.11: Ssp and corresponding sound propagation paths for the month of November in the condition of 0 to 15° launch angle with 0.5° step.

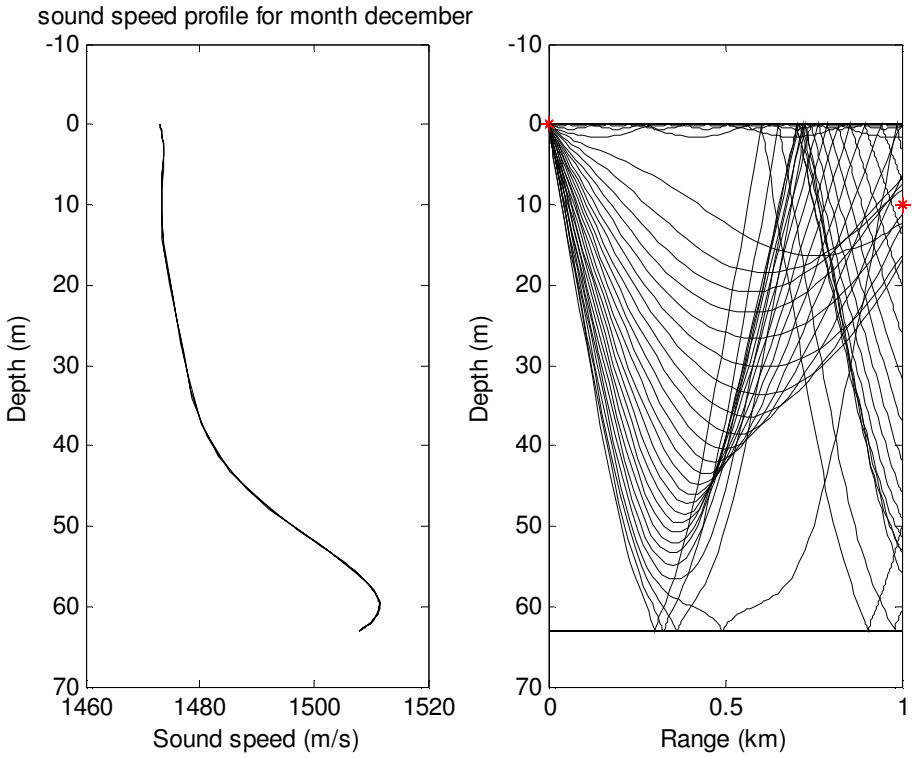

Figure C.12: Ssp and corresponding sound propagation paths for the month of December in the condition of 0.01 to 15° launch angle with 0.5° step.

APPENDIX D

Code for the Calculation of Sound Speed Profiles

In this section, the code which is used to calculate the sound speed profiles is given. As an example, code used for the calculation of the month of December is given.

speedformula.m

```
clear all
clc

load depth_temp_salinity_december.txt;

z=depth_temp_salinity_december(:,1);
T=depth_temp_salinity_december(:,2);
S=depth_temp_salinity_december(:,3);

% Medwin's formula for speed of sound (1975)
% Range of validity    0<=T<=35 degrees C
%                      0<=S<=45 ppt
%                      0<=z<=1000 m

c_Medwin=1449.2+4.6.*T-0.055.*(T.^2)+0.00029.*(T.^3)+…
            (1.34-0.01.*T).*(S-35)+0.016.*z;

% Mackenzie's formula for speed of sound (1981)
% Range of validity    -2<=T<=30 degrees C
%                      25<=S<=40 ppt
%                      0<=z<=8000 m

c_Mackenzie=1448.96+4.591.*T-5.304e-2.*(T.^2)+2.374e-4.*(T.^3)+...
                1.340.*(S-35)+1.630e-2.*z+1.675e-7.*(z.^2)-...
                1.025e-2.*(T.*(S-35))-7.139e-13.*(T.*(z.^3));

% Coppens's formula for speed of sound (1981)
% Range of validity    0<=T<=30 degrees C
%                      0<=S<=40 ppt
%                      0<=z<=4000 m
t=T/10;
```

```
c0=1449.05+45.7.*t-5.21.*(t.^2)+0.23.*(t.^3)+...
  (1.333-0.126.*t+0.009.*(t.^2)).*(S-35);

c_Coppens=c0+(16.23+0.253.*t).*(z/1000)+(0.213-0.1.*t).*((z/1000).^2)+...
              (0.016+0.0002.*(S-35)).*(S-35).*(t.*(z/1000));

% Chen and Millero's formula for speed of sound (1977)

C00=1402.388; C01=5.03830; C02=-5.81090e-2; C03=3.3432e-4;
C04=-1.47797E-6; C05=3.1419E-9; C10=0.153563; C11=6.8999E-4;
C12=-8.1829E-6; C13=1.3632E-7; C14=-6.1260E-10;C20=3.1260E-5;
C21=-1.7111E-6;C22=2.5986E-8;C23=-2.5353E-10; C24=1.0415E-12;
C30=-9.7729E-9; C31=3.8513E-10; C32=-2.3654E-12;

A00=1.389; A01=-1.262E-2; A02=7.166E-5; A03=2.008E-6; A04=-3.21e-8;
A10=9.4742E-5; A11=-1.2583E-5; A12=-6.4928E-8;A13=1.0515E-8;
A14=-2.0142E-10; A20=-3.9064E-7; A21=9.1061E-9; A22=-1.6009E-10;
A23=7.994E-12; A30=1.100E-10; A31=6.651E-12; A32=-3.391E-13;

B00=-1.922E-2; B01=-4.42E-5; B10=7.3637E-5; B11=1.7950E-7;

D00=1.727E-3; D10=-7.9836E-6;

% Converting Depth to Pressure
fi=41 %latitude
h_45=1.00818e-2.*z+2.465e-8.*(z.*2)-1.25e-13.*(z.*3)+2.8e-19.*(z.*4);
g=9.7803*(1+5.3e-3*sin(fi^2));
k=(g-2e-5.*z)./(9.80612-2e-5.*z);
h=h_45.*k;
h1=(0.01.*z)./(z+100)+6.2e-6.*z;  %common oceans between 60N and 40S
P=h-h1;

Cw =((C00 + C01.*T + C02.*T.^2 + C03.*T.^3 + C04.*T.^4 + C05.*T.^5) +...
       (C10 + C11.*T + C12.*T.^2 + C13.*T.^3 + C14.*T.^4).*P +...
       (C20 +C21.*T +C22.*T.^2 + C23.*T.^3 + C24.*T.^4).*P.^2 +...
       (C30 + C31.*T + C32.*T.^2).*P.^3);
A =((A00 + A01.*T + A02.*T.^2 + A03.*T.^3 + A04.*T.^4) +...
    (A10 + A11.*T + A12.*T.^2 + A13.*T.^3 + A14*T.^4).*P +...
    (A20 + A21.*T + A22.*T.^2 + A23.*T.^3).*P.^2 +...
    (A30 + A31.*T + A32.*T.^2).*P.^3);
B = B00 + B01.*T + (B10 + B11.*T).*P;
D = D00 + D10.*P;
c_ChenMillero=Cw + A.*S + B.*S.^(3/2) + D.*S.^2;

%Leroy's formula for speed of sound (1969)
% Range of validity     -2<=T<=34 degrees C
%                       ~20<=S<=42 ppt
%                       All depths in m

zeta=z/1000;   %depth in km
```

```
c_a=1e-1.*(zeta.^2)+2e-4.*(zeta.^2).*((T-18).^2)+1e-1.*zeta.*(fi/90);
c_b=2e-7.*T.*((T-10).^4);
c_c=-5e-4.*(zeta.^2).*((zeta-6).^2);
c_d=1.5e-3.*((S-35).^2).*(1-zeta);
c_0=1492.9+3.*(T-10)-(0.006.*(T-10).^2)-...
      0.04.*(T-18).^2+ 1.2.*(S-35)-0.01.*(T-18).*(S-35)+z./61;
c_Leroy=c_0+c_a+c_b+c_c+c_d;

%c_0 is the simlified formula
%c_0 + c_a + c_b is the basic formula
%c_c and c_d are corrections for z>7000 m and S<30
% the depth dependence in c_d is to fit Black Sea conditions

%Wilson's formula for speed of sound (1960)
% Range of validity     -4<=T<=30 degrees C
%                        0<=S<=37 ppt
%                        1<=P<=1000 kg/cm^2
Vt=4.5721*T-4.4532*0.01*(T.^2)-2.6045e-4*(T.^3)+7.9851e-6*(T.^4);
Vp=1.60272e-1*P + 1.0268e-5*P.^2 + 3.5216e-9*(P.^3) + 3.3603e-12*(P.^4);
Vs=1.39799*(S-35)+1.69202e-3*(S-35).^2;
Vstp=(S-35).*(-1.1244e-2.*T+7.7711e-7.*(T.^2)+7.7016e-5.*P-...
       1.2943e-7.*(P.^2)+3.158e-8.*P.*T+1.579e-9.*(P.*(T.^2)))+...
       P.*(-1.8607e-4*T+7.4812e-6*T.^2+4.5283e-8*T.^3)+...
      (P.^2).*(-2.5294e-7.*T+1.8563e-9.*(T.^2))-(P.^3).*(1.9646e-10.*T);
c_Wilson = 1449.14+ Vt+Vp+Vs+Vstp;

%Del Grosso's formula for speed of sound (1974)
% Range of validity     0<=T<=30 degrees C
%                       30<=S<=40 ppt
%                       0<=P<=1000 kg/cm^2
c_000 = 1402.392;
del_Ct=0.501109398873*10.*T-0.550946843172e-1.*(T.^2)+…
         0.22153596924e-3.*(T.^3);
del_Cs=0.132952290781e1.*S+0.128955756844e-3.*(S.^2);
del_Cp=0.156059257041.*P+0.244998688441e-4.*(P.^2)-…
         0.883392332513e-8.*(P.^3);
del_Cstp=-0.127562783426e-1.*(T.*S)+0.635191613389e-2.*(T.*P)+...
           0.265484716608e-7.*(T.^2).*(P.^2)-0.159349479045e-5.*(T.*(P.^2))+...
           0.522116437235e-9.*(T.*(P.^3))-0.438031096213e-6.*(P.*(T.^3))-...
           0.161674495909e-8.*(S.^2).*(P.^2)+0.96840315641e-4.*(S.*(T.^2))+...
           0.485639620015e-5.*(T.*(P.*(S.^2)))-0.340597039004e-3.*(T.*(S.*P));

c_DelGrosso=c_000 + del_Ct +del_Cs + del_Cp + del_Cstp;

titles={'c_Medwin','c_Mackenzie','c_Coppens','c_Chen-
Millero','c_Leroy','c_Wilson','c_DelGrosso'};
xlswrite('sound speed',titles,'december','A1')
xlswrite('sound speed',c_Medwin,'december','A2')
xlswrite('sound speed',c_Mackenzie,'december','B2')
xlswrite('sound speed',c_Coppens,'december','C2')
```

```
xlswrite('sound speed',c_ChenMillero,'december','D2')
xlswrite('sound speed',c_Leroy,'december','E2')
xlswrite('sound speed',c_Wilson,'december','F2')
xlswrite('sound speed',c_DelGrosso,'december','G2')
warning off MATLAB:xlswrite:AddSheet

figure(1)
plot(c_Medwin,z,c_Mackenzie,z,c_Coppens,z,c_ChenMillero,z,c_Leroy,z,c_Wilson,
z,c_DelGrosso,z)
set(gca,'ydir','reverse');
axis([1445 1515 0 70])
xlabel('Speed of Sound (m/s)')
ylabel('Depth (m)')
title('Sound Speed Profile for month December')
grid on
legend('Medwin','Mackanzie','Coppens','Chen-Millero','Leroy','Wilson','Del Grosso')
drawnow;
```

APPENDIX E

Ray Tracing Code

In this section, ray tracing code and functions which compute sound speed profiles and sound propagation paths with the source and the receiver are given. This code is modified from the ray tracing code written by Prof. Dr. Philippe Roux.

E.1: raytracing.m

```
clear all
pas=0.5;  teta0=0:pas:15;

%changing for every month according to the measured depth
%zbottom=60;  %for month january
zbottom=50;  %for month february & august
%zbottom=67;  %for month march
%zbottom=61;  %for months april & may & july & september
%zbottom=66;  %for month june
%zbottom=51;  %for month october
%zbottom=59;  %for month november
%zbottom=63;  %for month december

zsource=0;  zreceiver=10;  rfinal=1000;

freq=50;  T=1/freq;  lambda=1500/freq;

options = odeset('Events',@events);

for ii=1:length(teta0)
   taux=ii/length(teta0)

   z0=[zsource; tan(teta0(ii)*pi/180)];

   rstart=0;  rout = rstart;  zout = z0.';  timeout=0;

   while rout(end)~=rfinal

      [r,z]=ode45(@speed_der,[rstart rfinal],z0,options,zbottom);

      nt = length(r);  rout = [rout; r(2:nt)];  zout = [zout; z(2:nt,:)];
```

```
timeout=[0;cumsum(sqrt(diff(rout).^2+diff(zout(:,1)).^2)./speed(zout(2:end,1)))];
      z0(1)=z(nt,1);  z0(2)=-z(nt,2);  rstart = r(nt);
   end

   if abs(zout(end,1)-zreceiver)<lambda/3
      figure(1)
      subplot(1,2,2),plot(rout/1000,zout(:,1),'k')
      set(gca,'ydir','reverse');
      hold on
      subplot(1,2,2),plot(0,zsource,'r*')
      subplot(1,2,2),plot(rfinal/1000,zreceiver,'*r')
      subplot(1,2,2),plot(rout/1000,0*ones(1,length(rout)),'k')
      subplot(1,2,2),plot(rout/1000,zbottom*ones(1,length(rout)),'k')
      xlabel('Range (km)')
      ylabel('Depth (m)')
      drawnow;
   end
end
```

E.2: speed_der.m

```
function zdot = speed_der(r,z,zbottom)
zdot=zeros(2,1);

%sound speed equation and derivative for month January
% c=4.181e-10*z(1)^6-6.719e-07*z(1)^5+7.966e-05*z(1)^4-2.85e-03*z(1)^3+...
%       3.875e-02*z(1)^2-1.178e-01*z(1)+1463;
% der_c=25.086e-10*z(1)^5-33.595e-07*z(1)^4+31.864e-05*z(1)^3-...
%       8.55e-03*z(1)^2+7.75e-02*z(1)-1.178e-01;

%sound speed equation and derivative for month February
% c=5.37e-08*z(1)^6-7.959e-06*z(1)^5+4.848e-04*z(1)^4-1.448e-02*z(1)^3+...
%       2.186e-01*z(1)^2-1.583*z(1)+1461;
% der_c=32.22e-08*z(1)^5-39.795e-06*z(1)^4+19.392e-04*z(1)^3-...
%       4.344e-02*z(1)^2+4.372e-01*z(1)-1.583;

%sound speed equation and derivative for month March
% c=9.22e-09*z(1).^6-1.95e-06*z(1).^5+1.322e-04*z(1).^4-2.82e-03*z(1).^3-...
%       3.084e-03*z(1).^2+5.421e-01*z(1)+1451.22;
% der_c=55.327e-09*z(1).^5-9.75e-06*z(1).^4+5.288e-04*z(1).^3-...
%       8.4575e-03*z(1).^2-6.16774e-03*z(1)+5.42129e-01;

%sound speed equation and derivative for month April
% c=-1.74409e-08*z(1).^6+2.42827e-06*z(1).^5-1.28355e-04*z(1).^4+...
%       3.89526e-03*z(1).^3-5.458e-02*z(1).^2-3.432e-01*z(1)+1472.52;
% der_c=-10.4645e-08*z(1).^5+12.1414e-06*z(1).^4-5.13419e-04*z(1).^3+...
%       11.6858e-03*z(1).^2-10.9167e-02*z(1)-3.43239e-01;
```

```
%sound speed equation for month May
% c=-4.153e-08*z(1).^6+7.176e-06*z(1).^5-4.602e-04*z(1).^4+...
%       1.369e-02*z(1).^3-1.619e-01*z(1).^2-5.660e-01*z(1)+1487;
% der_c=-24.918e-08*z(1).^5+35.88e-06*z(1).^4-18.408e-04*z(1).^3+...
%       4.107e-02*z(1).^2-3.238e-01*z(1)-5.660e-01;

%sound speed equation for month June
%c=1500.66+2.8841*z(1)-1.47959*z(1).^2+0.268018*z(1).^3-.0248602*z(1).^4+...
%       0.00133485*z(1).^5-4.4056e-05*z(1).^6+9.0523e-07*z(1).^7-...
%       1.12459e-08*z(1).^8+7.70668e-11*z(1).^9-2.23075e-13*z(1).^10;
% der_c=2.8841-2.95917*z(1)+0.804053*z(1).^2-0.099441*z(1).^3+...
%       0.00667426*z(1).^4-2.64336e-04*z(1).^5+6.33661e-06*z(1).^6-...
%       8.99672e-08*z(1).^7+6.93601e-10*z(1).^8-2.23075e-12*z(1).^9;

%sound speed equation for month July
% c=3.15428e-13*z(1).^10-1.03054e-10*z(1)^9+1.41984e-08*z(1).^8-...
%       1.07038e-06*z(1).^7+4.79512e-05*z(1).^6-0.00130056*z(1).^5+...
%    0.0209598*z(1).^4-0.189898*z(1).^3+0.820581*z(1).^2-1.40364*z(1)+1515.17;
% der_c=3.15428e-12*z(1).^9-9.27487e-10*z(1).^8+1.13587e-07*z(1).^7-...
%       7.49264e-06*z(1).^6+2.87707e-04*z(1).^5-0.00650278*z(1).^4+...
%       0.0838391*z(1).^3-0.569695*z(1).^2+1.64116*z(1)-1.40364;

%sound speed equation for month August
 if z(1)<30
    c=-0.00144027*z(1).^3+0.0385051*z(1).^2-0.26721*z(1)+1512.3;
    der_c=-0.00432081*z(1).^2+0.0770102*z(1)-0.26721;
 else
    c=5.02484e-06*z(1).^6-0.00130359*z(1).^5+0.140725*z(1).^4-...
       8.08734*z(1).^3+260.781*z(1).^2-4469.35*z(1)+33262.2;
    der_c=3.0149e-05*z(1).^5-0.00651795*z(1).^4+0.562899*z(1).^3-...
      24.262*z(1).^2+521.563*z(1)-4469.35;
 end

%sound speed equation for month September
% c=8.563e-08*z(1).^6-1.549e-05*z(1).^5+1.018e-03*z(1).^4-...
%       2.887e-02*z(1).^3+3.310e-01*z(1).^2-1.534*z(1)+1509;
% der_c=51.378e-08*z(1).^5-7.745e-05*z(1).^4+4.072e-03*z(1).^3-...
%       8.661e-02*z(1).^2+6.62e-01*z(1)-1.534;

%sound speed equation for month October
% if z(1)<23
% c=-0.000382784*z(1).^3-0.000171436*z(1).^2+0.156438*z(1)+1499.;
% der_c=-0.00114835*z(1).^2-0.000342871*z(1)+0.156438;
% else
% c=0.00000447878*z(1).^5-0.000165002*z(1).^4-0.0426743*z(1).^3+...
%       3.71319*z(1).^2-106.657*z(1)+2522.89;
% der_c=0.0000223939*z(1).^4-0.000660009*z(1).^3-...
%       0.128023*z(1).^2+7.42638*z(1)-106.657;
% end
```

```
%sound speed equation for month November
% c=9.872e-09*z(1).^6-2.153e-06*z(1).^5+1.611e-04*z(1).^4-...
%       5.029e-03*z(1).^3+6.926e-02*z(1).^2-3.347e-01*z(1)+1483;
% der_c=59.232e-09*z(1).^5-10.765e-06*z(1).^4+6.444e-04*z(1).^3-...
%       15.087e-03*z(1).^2+13.852e-02*z(1)-3.347e-01;

%sound speed equation for month December
% c=-3.857e-08*z(1).^6+6.235e-06*z(1).^5-3.680e-04*z(1).^4+...
%      9.920e-03*z(1).^3-1.147e-01*z(1).^2+4.866e-01*z(1)+1473;
% der_c=-23.142e-08*z(1).^5+31.175e-06*z(1).^4-14.72e-04*z(1).^3+...
%      29.76e-03*z(1).^2-2.294e-01*z(1)+4.866e-01;

zdot(1)=z(2);
zdot(2)=(1+z(2)^2)*(-der_c/c);
```

E.3: speed.m

```
function c=speed(z)
%sound speed equation for month January
% c=4.181e-10*z.^6-6.719e-07*z.^5+7.966e-05*z.^4-2.85e-03*z.^3+...
%       3.875e-02*z.^2-1.178e-01*z+1463;

%sound speed equation for month February
% c=5.37e-08*z.^6-7.959e-06*z.^5+4.848e-04*z.^4-1.448e-02*z.^3+...
%       2.186e-01*z.^2-1.583*z+1461;

%sound speed equation for month March
% c=9.22e-09*z.^6-1.95e-06*z.^5+1.322e-04*z.^4-2.82e-03*z.^3-...
%     3.084e-03*z.^2+5.421e-01*z+1451.22;

%sound speed equation for month April
% c=-1.74409e-08*z.^6+2.42827e-06*z.^5-1.28355e-04*z.^4+3.89526e-03*z.^3-...
%       5.458e-02*z.^2-3.432e-01*z+1472.52;

%sound speed equation for month May
% c=-4.153e-08*z.^6+7.176e-06*z.^5-4.602e-04*z.^4+1.369e-02*z.^3-...
%       1.619e-01*z.^2-5.660e-01*z+1487;

%sound speed equation for month June
% c=1500.66+2.8841*z-1.47959*z.^2+0.268018*z.^3-0.0248602*z.^4+...
%       0.00133485*z.^5-4.4056e-05*z.^6+9.0523e-07*z.^7-1.12459e-08*z.^8+...
%       7.70668e-11*z.^9-2.23075e-13*z.^10;

%sound speed equation for month July
% c=3.15428e-13*z.^10-1.03054e-10*z.^9+1.41984e-08*z.^8-1.07038e-06*z.^7+...
%       4.79512e-05*z.^6-0.00130056*z.^5+0.0209598*z.^4-0.189898*z.^3+...
%       0.820581*z.^2-1.40364*z+1515.17;
```

```
%sound speed equation for month August
 if z<30
 c=-0.00144027*z.^3+0.0385051*z.^2-0.26721*z+1512.3;
 else
 c=5.02484e-06*z.^6-0.00130359*z.^5+0.140725*z.^4-8.08734*z.^3+...
     260.781*z.^2-4469.35*z+33262.2;
 end

%sound speed equation for month September
% c=8.563e-08*z.^6-1.549e-05*z.^5+1.018e-03*z.^4-2.887e-02*z.^3+...
%       3.310e-01*z.^2-1.534*z+1509;

%sound speed equation for month October
% if z<23
% c=-0.000382784*z.^3-0.000171436*z.^2+0.156438*z+1499.;
% else
% c=0.00000447878*z.^5-0.000165002*z.^4-0.0426743*z.^3+...
%       3.71319*z.^2-106.657*z+2522.89;
% end

%sound speed equation for month November
% c=9.872e-09*z.^6-2.153e-06*z.^5+1.611e-04*z.^4-5.029e-03*z.^3+...
%       6.926e-02*z.^2-3.347e-01*z+1483;

%sound speed equation for month December
% c=-3.857e-08*z.^6+6.235e-06*z.^5-3.680e-04*z.^4+9.920e-03*z.^3-...
%       1.147e-01*z.^2+4.866e-01*z+1473;

       subplot(1,2,1),plot(c,z,'k')
       axis([1445 1515 -10 70])  %changing for every month according to the ray
tracing figure
       set(gca,'ydir','reverse');
       xlabel('Sound speed (m/s)')
       ylabel('Depth (m)')
       title('sound speed profile for month august')
       drawnow;
```

E.4: events.m

```
function [value,isterminal,direction] = events(r,z,zbottom)

value = [z(1); z(1)-zbottom];     % detect height = 0
isterminal = [1; 1];   % stop the integration
direction = [-1; 1];   % negative direction
```

RESUME

Sevil Deniz Yakan was born in 1982 in the city of Ordu. She completed her secondary school education in Büyükşehir Hüseyin Yıldız Anatolian High School in Büyükçekmece, Istanbul. Later, she continued her education in Erenköy High School for Girls in Erenköy, Istanbul and graduated with high honours degree ranking first. Afterwards, she began her education in Istanbul Technical University, Faculty of Naval Architecture and Ocean Engineering in 2000, and graduated with high honours degree by ranking first in her department in 2005. At present, she continues her education in Istanbul Technical University, Institute of Science and Technology, Ocean Engineering Program and working as a research assistant at Naval Architecture and Ocean Engineering Faculty, Oceanography Division.